Short-range-order diffuse scattering in decagonal Ni-rich Al-Ni-Co quasicrystals

Akiji Yamamoto
National Institute for Materials Science, Namiki 1, Tsukuba, Ibaraki, 305-0044, Japan
(Received 8 September 2010; revised manuscript received 21 February 2011; published 12 May 2011)

An analytical expression of the diffuse scattering (DS) intensity due to short-range order derived in a recent paper [A. Yamamoto, Acta Crystallogr. Sect. **A 66**, 372 (2010)] is applied to analyze DS intensities of the S1 phase at 1120 K and the quenched basic Ni rich (b-Ni) phase in decagonal $Al_{70}Ni_{22}Co_8$ (d-$Al_{70}Ni_{22}Co_8$) quasicrystals. The analysis is based on a microdomain model consisting of 20 Å clusters. The S1 and b-Ni phases are low- and high-temperature phases of d-$Al_{70}Ni_{22}Co_8$ so that microdomains with the S1 phase structure are assumed to be formed in the b-Ni phase and vice versa. The intercluster correlation of the 20 Å clusters within the microdomains is assumed to be the same as that in a corresponding completely ordered structure up to the third intercluster distance $\simeq$32 Å. It is demonstrated that simulated DS intensity distributions reproduce characteristic features in the observed DS intensity in these phases. This suggests that the analysis of DS intensity is efficient for understanding phase transition mechanisms of quasicrystals. It also shows the effectiveness of the theory and applicability of cluster-based DS intensity calculations to real quasicrystals, which reduce the number of short-range-order parameters drastically.

DOI: 10.1103/PhysRevB.83.184203 PACS number(s): 61.05.cc, 61.05.cp, 61.44.Br, 61.50.Ah

I. INTRODUCTION

In quasicrystals, it is known that there exists diffuse scattering (DS) due to random phasons together with the DS due to phonons. These two are called the phason diffuse scattering (PDS) and the thermal diffuse scattering (TDS). The former is specific to quasicrystals and its nature is theoretically investigated.[1–3] This is observed in close vicinity to Bragg reflections similarly to the DS by phonons. They are caused by a long-range correlation of the fluctuation of atom positions. The theory of PDS was applied to icosahedral Al-Pd-Mn (i-Al-Pd-Mn), decagonal Al-Ni-Co (d-Al-Ni-Co), and d-Al-Ni-Fe quasicrystals.[4–6] In conventional crystals, a solid solution shows DS with a different origin. This is caused by a statistical distribution of different atoms which occupy an atom site. The correlation length in this case is usually short and therefore this is called short-range-order diffuse scattering (SRODS). Recently a theory of SRODS in quasicrystals was given by the author.[7]

Since most quasicrystals are alloys (solid solutions in metals), SRODS is generally expected. A variety of DS intensity distributions have been observed in d-Al-Ni-Co and d-Al-Ni-Fe quasicrystals as expected, which depend on their chemical composition and/or thermal history.[8–12] In i-Al-Pd-Mn quasicrystals, PDS is very strong but they are expected also to show SRODS.[4,13,14] The intensity distribution of SRODS is determined by the correlation function of the fluctuation of atomic scattering factors (or scattering lengths of neutron) from their average value. In order to demonstrate the effectiveness of the theory of SRODS in solid state physics, we apply this theory to that of d-Al-Ni-Co quasicrystals to obtain information on the phase transformation mechanism in quasiperiodic structures. For simplicity, SRODS is simply called DS hereafter.

Decagonal quasicrystals have a period c along the tenfold axis, so that their diffraction pattern has a period $c^* = 1/c$ along this direction. An important feature of DS in decagonal quasicrystals is that the DS intensity exists only on Bragg reflection planes normal to the tenfold axis. In some cases, however, DS is observed at the midpoint of two Bragg reflection planes without accompanying Bragg reflection. Even in this case, DS intensity appears only on the plane. The former suggests that the correlation length of a quasicrystal along the tenfold axis is very large, while the latter implies that there is a short-range order related to a superstructure with a doubled period. In this paper, we consider the former case where a quasicrystal is assumed to have a complete period along the tenfold axis, although real b-Ni and S1 phases show DS intensity at the midpoint of two Bragg reflection planes.

$Al_{70}Ni_{22}Co_8$ gives a diffraction pattern consistent with the decagonal symmetry at high temperatures but shows satellite reflections indicating a quasicrystalline superstructure phase[15] at lower temperatures.[16,17] The higher and lower temperature phases are called the basic Ni rich (b-Ni) phase and the S1 phase, respectively. The structure of the b-Ni phase is determined by x-ray diffraction[18,19] and the space group of this structure is determined to be $P10_5/mmc(10^71mm)$. (In this paper the space group and point group symbols recommended by IUCr are employed.[20,21]) A structure refinement of the S1 phase has not been performed yet but from high-resolution transmission electron microscopy (HRTEM) observations and $5D$ modeling, it is considered that this phase consists of so-called 20 Å (columnar) clusters showing fivefold symmetry ($5f$ clusters) in the innermost shell.[22–24] The true symmetry of the 20 Å clusters is however not fivefold symmetric and they have only mirror symmetry.

In both phases, there exists DS which strongly depends on the sample temperature in high temperature experiments or the quenching temperature in room temperature experiments as mentioned below. The DS of the b-Ni phase with chemical composition $Al_{72}Ni_{20}Co_8$ quenched at 1073 K differs from that at temperature 1116 K.[10] Very clear temperature dependent DS is also observed in the S1 phase with chemical composition of $Al_{70}Ni_{17}Co_{13}$ measured at 300 K and 1120 K.[5,25] These experimental evidences indicate that local structural fluctuations of these phases from their average structures strongly depend on

temperature and thermal history and suggest that the analysis of DS intensity near the phase transition temperature T_c provides important information on the intra-quasi-crystalline phase transition mechanism. In this paper, the theory of DS in quasicrystals is applied to the b-Ni and S1 phases for the first time. The analysis of DS clarifies that medium-range correlation of the order of 30 Å is developed near T_c. Thus we can confirm by the analysis of the DS intensity as shown below that the phase transition occurs by the creation of microdomains near T_c. Therefore this provides a new way for investigating phase transition mechanisms in quasiperiodic structures, which are not clarified yet.

In a previous paper[24] a model with the color space group $P10_5/mc'm'(10^71mm)$ has been proposed for the S1 phase. (The prime means an antisymmetric operator, which is combined with the rotation and time-reversal operations.) In this phase, there are 20 $5f$ clusters which are obtained from two basic clusters by the symmetry operation in the point group $\bar{5}(\bar{5}^2)$. On the other hand, the b-Ni phase consists of ten clusters with mirror symmetry (m clusters).[24,26] The ten clusters are also obtained from one basic cluster by $\bar{5}(\bar{5}^2)$.

In the b-Ni phase of d-$Al_{70}Ni_{22}Co_8$ quenched from 1073 K, which is 81 K above the phase transition temperature ($T_c \simeq 992$ K), broad peaks are observed around strong Bragg reflections and they are attributed to the satellite reflections in the S1 phase.[9,10] It is known that the correlation length of the DS estimated from FWHM of the broad peaks are about 28 Å.[10] To analyze the broad peaks therefore, we need to consider the correlation up to this distance. In such a case, if we consider the correlation of each atom, the number of short-range order parameters (so-called α parameters[27]) becomes large, because there are many atoms within the correlation length from an atom, and many independent inter-atomic distances. If we can consider that the correlation within the 20 Å cluster is complete, the number of intercluster correlation parameters will be small. However even after this simplification, the DS intensity analysis of the d-Al-Ni-Co is not straightforward because of the following reasons.

These clusters are situated at fixed positions in ideal structures in the b-Ni and S1 phases. There are ten cluster sites in the b-Ni phase, each of which is occupied by one of the ten clusters as shown later. Similarly, there are 50 sites in the S1 phase, which are occupied by one of the 20 clusters. Therefore if we consider a disordered structure in these phases, it is conceivable that one cluster site among 10 or 50 sites is occupied by one of the 30 clusters. This corresponds to a case in the DS in conventional crystals where there are 10 or 50 sites in a unit cell and each atom site is occupied by one of 30 atom species.[7] Kobas *et al*. analyzed the DS of the S1 phase assuming that some site is randomly occupied by the ten m clusters of the b-Ni phase.[5] In this analysis, the contribution of the $5f$ clusters to the DS is not taken into account. In this paper, we consider a simple case where three clusters (two $5f$ and one m cluster) among 30 clusters occupy each cluster site statistically, although the triplets of the clusters are different depending on the sites. The purpose of the paper is to clarify the origin of the DS based on such a model which will be closely related to the phase-transition mechanism and to show the efficiency of the cluster-based DS theory.

The arrangement of this paper is as follows. The structure models of the S1 and b-Ni phases proposed previously are summarized in Sec. II. The phase transition of the S1 phase to the b-Ni phase and their structural change are written in Sec. III. To consider the correlation between 20 Å clusters, the correlation of the clusters in the completely ordered structures in both phases is discussed in Sec. IV. The DS intensity theory in quasicrystals is summarized in Sec. V. The correlation of clusters used in the DS intensity calculations is described in Sec. VI. Finally DS intensity distributions of the S1 and b-Ni phases are analyzed in Sec. VII.

II. S1 AND B-NI PHASES

We use two coordinate systems to describe structures of the b-Ni and S1 phases. They are related with a transformation matrix T written in Appendix A. The lattice constant a_0 of the b-Ni phase is $\simeq 2.7$ Å while that of the S1 phase is $a = 2\cos(\pi/10)a_0 \simeq 5.2$ Å. The lattice constant c (period along the tenfold axis) is $\simeq 4.0$ Å in both phases.[24] The coordinates with respect to the former and latter phases are denoted as $(x_1,x_2,x_3,x_4,x_5)_0$ and (x_1,x_2,x_3,x_4,x_5). The external (physical) and internal (complementary) space components of a 5D vector are represented by the superscripts e and i. We consider only x-ray DS, for which the distribution of Al and transition metal (TM) atoms are relevant to the scattering intensity. (Two TMs, Ni and Co, are not distinguished from each other since it is difficult to discriminate them by a conventional x-ray diffraction experiment.)

The independent occupation domains (ODs) and the atom arrangement of the S1 phase are shown in Figs. 1 and 2. The so-called 20 Å cluster includes atoms in a decagon in Fig. 2 and a part of small ten pentagons around it. The radius of the cluster (a distance between the centers of a decagon and a pentagon around it) is about 10 Å($\tau^3 a_0 \simeq 10.2$ Å). Adjacent two 20 Å clusters share two pentagons when they are distant by 20 Å($2\tau^3 a/\sqrt{5} \simeq 19.7$ Å). The nearest decagon distance is about 12 Å($2\tau^2 a/\sqrt{5} \simeq 12.2$ Å). Then they are slightly

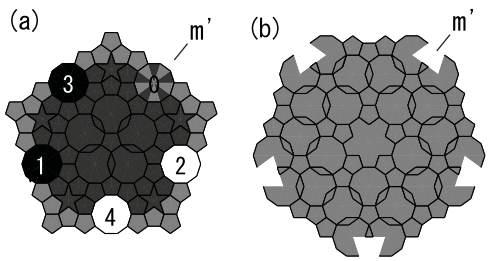

FIG. 1. Independent occupation domains (ODs) of a model of the S1 phase with the color space group $P10_5/mc'm'(10^71mm)$, which are located at (a) $(0,2,-1,1,5z)/5$ and (b) $(0,4,-2,2,5z)/5$ ($z = 1/4$). [These two positions are represented by the coordinates $(1,1,1,1,5z)_0/5$ and $(2,2,2,2,5z)_0/5$ in the b-Ni phase.] White and black domains are occupied by colored Al and transition metal (TM) atoms, while light and dark gray ones are occupied by gray Al and TM atoms. Decagonal ODs labeled 0-4 and the corresponding decagonal ODs in the inverted OD located at $-(0,2,-1,1,5z)/5$ create the atom positions of the first shell in the 20 Å clusters in Fig. 2.

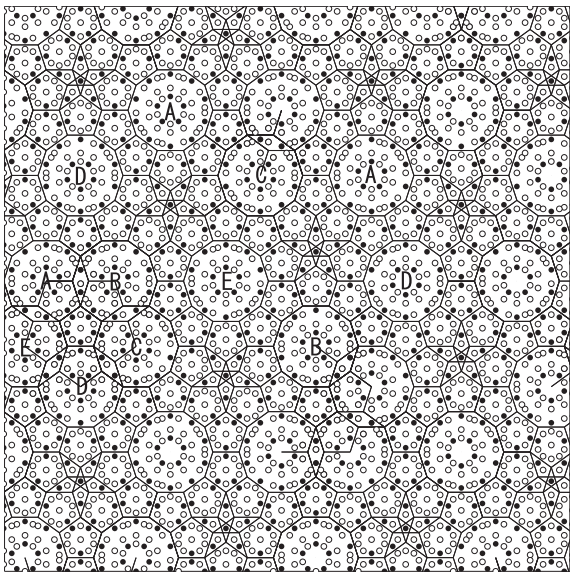

FIG. 2. Structure of the S1 phase, which is projected along the tenfold axis. Solid and open circles denote transition metal (Ni or Co) and Al atoms, respectively. The labels E, A, B, C, and D indicate that the cluster centers are generated by the decagonal ODs at the site $(s,s,s,s,5z)/5$ ($s = 0,1,2,3,4$) shown in Fig. 5.

overlapped. In the phase transition from the b-Ni phase to the S1 phase, the atom arrangement only in a decagon is considered to be changed as is summarized in the next section.

The b-Ni phase has a cluster arrangement similar to that of the S1 phase but each cluster position is occupied by a different cluster as seen in Fig. 3. The cluster centers in both phases form the Penrose pentagon tiling (PPT) with an edge length of about 20 Å.[24]

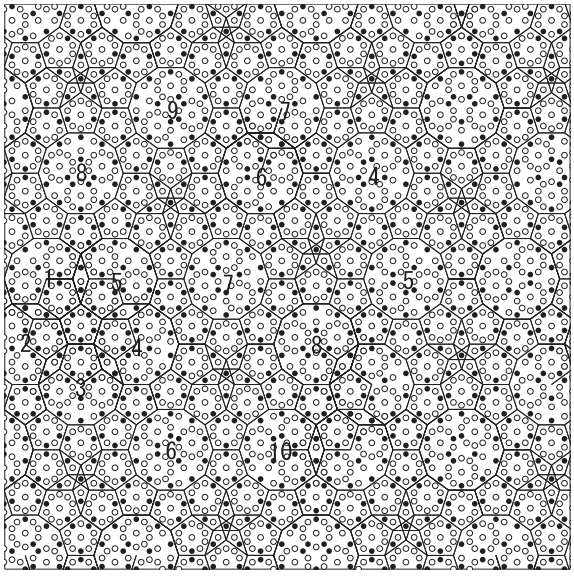

FIG. 3. Structure of the b-Ni phase, which is projected along the tenfold axis. Solid and open circles stand for transition metal (Ni or Co) and Al atoms. The labels 1-10 represent that the cluster centers are generated by triangles with the same number in Fig. 5(a).

III. PHASE TRANSITION BETWEEN B-NI AND S1 PHASES

In an ideal model of the S1 phase given by the ODs in Fig. 1, the clusters are perfectly ordered. One of the two $5f$ clusters [Figs. 4(a) and 4(b)] and clusters equivalent to them by symmetry operators R_5^{k-1} and IR_5^{k-1} ($1 \leqslant k \leqslant 5$) are located at each vertex of the PPT with an edge length of about 20 Å, where R_5 and I are fivefold rotation and inversion operators. [They are the generators of the point group $\bar{5}(\bar{5}^2)$.] The inner-most shells of the $5f$ clusters in Figs. 4(a) and 4(b) have different orientations. We call them down and up orientations, although the $5f$ clusters have no true fivefold symmetry because of their mirror symmetry in the outermost shells. The cluster arrangement has a preference so that the two clusters apart by 20 Å are of different orientations.[23] The clusters on the pentagon in the PPT cannot obey this preference completely because the PPT includes many pentagons and a pair of clusters among five pairs linked by edges of the pentagon has to be the same orientation. If different cluster orientations in such a pair are preferred energetically, this system is energetically frustrated. Then we can easily expect that some kind of disorder exists in this system. We take, however, a perfectly ordered model [24] as a basis of the analysis of DS intensity and consider fluctuation from this structure.

In a completely ordered model of the S1 phase, sharp superstructure (satellite) reflections are observed in its diffraction patterns without accompanying DS, although TDS around each Bragg spot is expected. Near the transition temperature (T_c) to the b-Ni phase, however, we may expect the dissolution of the $5f$ clusters [Figs. 4(a) and 4(b)] and the creation of the m cluster [Fig. 4(d)]. In fact such a change in clusters has been observed.[23] This will cause the DS.

The structure analysis of the b-Ni phase suggests that this phase consists only of the m clusters.[28] One kind of m cluster with ten different orientations is located at a fixed position

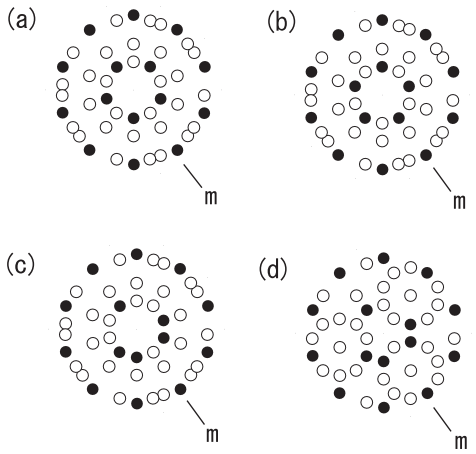

FIG. 4. Two clusters in a decagon in the model of the S1 phase shown in Fig. 2, (a) and (b), and that of the b-Ni phase, (d). The former is obtained from the latter by the interlayer phason flip via the intralayer phason flip state (c).[24] The clusters in (a) and (b) are called $5f$ clusters while that in (d) is m cluster. Their symmetry is both m. The position of the mirror plane is denoted by m. Note that the atom arrangement of the outermost shells in (a) and (b) breaks the fivefold symmetry.

depending on the location of the cluster and it is completely ordered in an ideal b-Ni structure. In a detailed examination of synchrotron radiation data, however, broad peaks located at the satellite reflection position are found in the quenched b-Ni phase and b-Ni phase near T_c to the S1 phase.[9,10] In this case it is conceivable that there exists the $5f$-cluster arrangement seen in the S1 phase within a short range in the b-Ni phase. Therefore it may be considered that at higher temperatures all the $5f$ clusters disappear and only the m clusters exist, while near T_c, a part of the m clusters is dissolved and the $5f$ clusters are created.

There are 20 $5f$ clusters and ten m clusters in total. They are obtained from those in Figs. 4(a), 4(b), and 4(d) by applying symmetry operations of the point group $\bar{5}(\bar{5}^2)$ as mentioned above. In the following, we assume that the m cluster shown in Fig. 4(d) dissolves and creates the cluster shown in Fig. 4(a) or 4(b) and vice versa in the phase transition between the S1 and b-Ni phases. In the structural change from the structure in Fig. 4(d) to that in Fig. 4(a), the number of necessary TM and Al flips in the innermost ten atoms via the intermediate state shown in Fig. 4(c) is 2, while in the change between Figs. 4(d) and 4(b), it is 4. Additional six Al atom jumps have to be accompanied in both cases to obtain the Al position in the outermost shell in Figs. 4(a) and 4(b). They are called the interlayer and intralayer phason flips in a previous paper.[24] This suggests that the phase transition between the two phases does not necessitate long-range atom diffusion. From the above considerations, we can expect that the phase transition occurs due to the interlayer and intralayer phason flips, which causes the creation of the m clusters in the S1 phase accompanied by the dissolution of the $5f$ clusters, while in the b-Ni phase the creation of the $5f$ clusters is accompanied by the dissolution of the m clusters.

Noting Al and TM arrangement in the innermost shell, two orientations of the $5f$ cluster shown in Figs. 4(a) and 4(b) are called down and up orientations for simplicity. In total, there are ten up and ten down orientation $5f$ clusters. (Note that the inverted cluster is said as a cluster with a different orientation in this paper.) We consider 20 clusters obtained from Figs. 4(a) and 4(b) by the symmetry operations R_5^{k-1} $(1 \leqslant k \leqslant 5)$ and $I R_5^{k-6}$ $(6 \leqslant k \leqslant 10)$. The former ten [obtained from Fig. 4(a)] are called C_k^{5f} clusters and the latter ten are called $C_k'^{5f}$ clusters $(1 \leqslant k \leqslant 10)$. Among them, C_k^{5f} $(1 \leqslant k \leqslant 5)$ and $C_k'^{5f}$ $(6 \leqslant k \leqslant 10)$ are of down orientation, while C_k^{5f} $(6 \leqslant k \leqslant 10)$ and $C_k'^{5f}$ $(1 \leqslant k \leqslant 5)$ are of up orientation, respectively. Similarly the clusters obtained from Fig. 4(d) by the same symmetry operators are called C_k^m clusters $(1 \leqslant k \leqslant 10)$.

IV. ARRANGEMENT OF CLUSTERS IN COMPLETELY ORDERED STRUCTURES

In order to analyze the DS in the S1 or b-Ni phase, two $5f$ and one m cluster, and their orientations have to be considered. We neglect the difference in the structures between the S1 and b-Ni phases other than the difference in these clusters and their orientations, assuming that the other atoms have complete chemical order. Since the completely ordered parts do not contribute to the DS, we can only consider the swap of m and $5f$ clusters and their orientational disordering in the calculation of the DS intensity. In this section, the cluster arrangements of these clusters in ideal models of the S1 and b-Ni phases are described.

A. Cluster arrangement in ideal structure models

In 5D models of the b-Ni and S1 phases proposed in a previous paper,[24] cluster centers are generated by the decagon with a radius of $2\tau^{-3}a/\sqrt{5}$ (Fig. 5) situated at $\mathbf{x}_i = (i,i,i,i,5z)/5$ $(i = 0,1,\ldots,4)$. We call these E, A, B, C, and D sites and ODs located there, E, A, B, C, and D ODs. Similarly the vertices in the PPT generated by these ODs are called E, A, B, C, and D vertices and clusters centered at these positions E, A, B, C, and D clusters hereafter. The vertices generated by each OD are classified into ten subclasses, which are generated by ten triangles in E, A, B, C, or D OD. (See Fig. 5.)

Cluster centers occupied by an m cluster with a fixed orientation in the b-Ni phase are created by a subdivided OD shown in Fig. 5. (See Appendix B.) Each fin (triangle) of the pinwheel-shaped OD in the figure generates the cluster center positions where the clusters with the same orientations (including the orientation of the outermost shell) are located. At the vertices created by OD 1 in Fig. 5(a), the m cluster shown in Fig. 4(d) is located. On the other hand, the clusters with the orientation which is obtained from Fig. 4(d) by the rotation operator R_5^{k-1} is located at the positions generated by ODs k $(1 \leqslant k \leqslant 5)$. Similarly, the position generated by ODs k $(6 \leqslant k \leqslant 10)$ are occupied by the clusters which are obtained

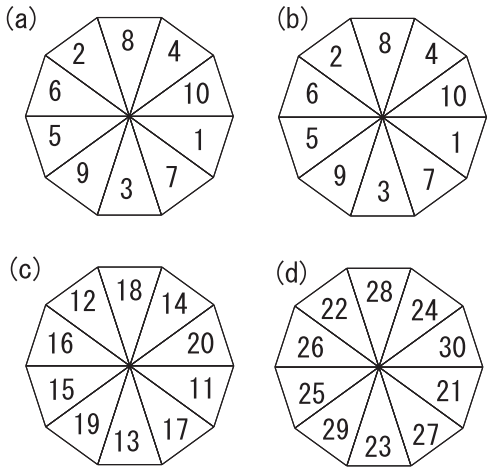

FIG. 5. Occupation domains of the cluster centers for the b-Ni phase (a) and for the S1 phase (b-d). The horizontal and vertical directions are parallel to $\mathbf{a}_4$ and $\mathbf{a}_5$ of the S1 phase. The radius of the decagon is $\tau^{-4}\sqrt{5}a_0/2$ $(= 2\tau^{-3}a/\sqrt{5})$ with $a_0 = 2.73$ Å$[\tau = (1+\sqrt{5})/2]$. The center of the decagon in (a) is located at $(s,s,s,s,5z)/5$ $(s = 0,1,2,3,4)$ in the unit cell of the S1 phase. These decagons generate the vertices of the pentagon Penrose tiling (PPT) with an edge length of $2\tau^3 a/\sqrt{5} \simeq 19.7$Å. In an ideal b-Ni structure, the m cluster with the same orientation is located at the positions generated by ODs with the same label independent of s. Three independent ODs in the S1 phase centered at $(0,0,0,0,5z)/5$, $(1,1,1,1,5z)/5$, and $(2,2,2,2,5z)/5$ are shown in (b), (c), and (d). (These sites are referred to as E, A, and B sites in the text.) A different triangular region in the subdivided ODs generates cluster centers occupied by a different cluster.

TABLE I. The cluster distribution of 20 $5f$ clusters in the S1 phase (the first five lines) and ten m clusters in the b-Ni phase (the last line). The symbols C_k^{5f} and $C_k'^{5f}$ $(1 \leqslant k \leqslant 5)$ denote the clusters which are obtained from those in Figs. 4(a) and 4(b) by R_5^{k-1}, where R_5 is the fivefold rotation operator. The symbols C_k^{5f} and $C_k'^{5f}$ $(6 \leqslant k \leqslant 10)$ represent inverted clusters of C_k^{5f} and $C_k'^{5f}$ $(1 \leqslant k \leqslant 5)$ by I, where I denotes the inversion operator. Similarly, C_k^m $(1 \leqslant k \leqslant 5)$ denote the clusters which are obtained from Fig. 4(d) by R_5^{k-1} while C_k^m $(6 \leqslant k \leqslant 10)$ by IR_5^{k-6}. In the b-Ni phase, the site A_k, B_k, C_k, D_k, and E_k are translationally equivalent, so that they are occupied by the same clusters as in E_k which are shown in the last line.

site	A_k $(1 \leqslant k \leqslant 5)$	A_k $(6 \leqslant k \leqslant 10)$
cluster	C_k^{5f}	$C_k'^{5f}$
site	B_k $(1 \leqslant k \leqslant 5)$	B_k $(6 \leqslant k \leqslant 10)$
cluster	C_k^{5f}	$C_k'^{5f}$
site	C_k $(1 \leqslant k \leqslant 5)$	C_k $(6 \leqslant k \leqslant 10)$
cluster	$C_k'^{5f}$	C_k^{5f}
site	D_k $(1 \leqslant k \leqslant 5)$	D_k $(6 \leqslant k \leqslant 10)$
cluster	$C_k'^{5f}$	C_k^{5f}
site	E_k $(1 \leqslant k \leqslant 5)$	E_k $(6 \leqslant k \leqslant 10)$
cluster	C_k^{5f}	C_k^{5f}
site	E_k $(1 \leqslant k \leqslant 5)$	E_k $(6 \leqslant k \leqslant 10)$
cluster	C_k^m	C_k^m

from Fig. 4(d) by IR_5^{k-6}. The cluster shown in Fig. 4(a) is transformed into that in Fig. 4(b) by time-reversal operation E' provided that the Al and TM atoms in the innermost shell are colored atoms.[29]

The triangles for the ODs E, A, etc., are represented by subscripts k within a range $1 \leqslant k \leqslant 10$. In this notation, the ODs 1-10 in Fig. 5(b) are denoted as ODs E_1-E_{10}, while the ODs 11-20 in Fig. 5(c) as ODs A_1-A_{10} and so on. Similarly, the vertices, generated by these ODs are called the E_k and A_k vertices for convenience.

In the b-Ni phase, the five sites A-E are translationally equivalent, since $\mathbf{x}_i$ $(i = 1,2,\ldots,5)$ are equal to $(0,0,i,0,z)_0$, that is, lattice vectors of the b-Ni phase (Appendix A). Their site symmetry is $\bar{1}0m2$ for all sites, since all ODs (atoms) are on the mirror plane normal to the tenfold axis ($z = \pm 1/4$). On the other hand, the clusters located at these vertices have only mirror symmetry. (Note that there exist another mirror plane including the tenfold axis.) The vertices generated by ODs E_k, A_k, B_k, C_k, and D_k $(1 \leqslant k \leqslant 10)$ are occupied by the cluster C_k^m in the completely ordered b-Ni structure. The location of all clusters in the b-Ni phase is given in the last rows of Table I.

In the S1 phase, the E, A, and B sites are independent, while the D and C sites are related with the A and B sites by the inversion, I. In an ideal model of the S1 phase,[24] the sites A_k and B_k $(1 \leqslant k \leqslant 10)$ are occupied by C_k^{5f} $(1 \leqslant k \leqslant 5)$ and $C_k'^{5f}$ $(6 \leqslant k \leqslant 10)$, which all have up orientation. Similarly, the sites C_k and D_k $(1 \leqslant k \leqslant 10)$ are occupied by down orientation $C_k'^{5f}$ $(1 \leqslant k \leqslant 5)$ and C_k^{5f} $(6 \leqslant k \leqslant 10)$. In addition, ODs E_k are occupied by up orientation C_k^{5f} for $1 \leqslant k \leqslant 5$ and down orientation C_k^{5f} for $6 \leqslant k \leqslant 10$. The the clusters at the sites $C_{k\pm5}$ and $D_{k\pm5}$ are related by the inversion I to those at the sites B_k and A_k. The location of all clusters in the S1 phase is listed in Table I.

B. Antiphase domains

We consider domain structures in the S1 phase, which will appear in the b-Ni phase. Two kinds of antiphase domains described below can be considered in the S1 phase. There is a structure which is obtained from the S1 structure mentioned above by swapping Al and TM in the innermost shell of clusters shown in Figs. 4(a) and 4(b), where C_k^{5f} and $C_k'^{5f}$ are swapped. Then all the clusters with up orientation are replaced by those with down orientation and vice versa. If we consider that Al and TM atoms in the innermost shell of the cluster in Figs. 4(a) and 4(b) are colored atoms, the color symmetries of these two structures are both given by $P10_5/mc'm'$.[24] Using the color symmetry operation, these two clusters are interchanged by the time-reversal operator, E'. In a completely ordered S1 phase, one of the two structures is realized. Near T_c however, the two domains may coexist with a different volume ratio. In this case, the two domains are related by E', so that they are called *antisymmetric domains*. This can be recognized as a kind of the *antiphase domains* in quasicrystals.

There is another kind of antiphase domain, which is related with the origin shift. In the b-Ni phase, the sites E, A, B, C, and D are translationally equivalent, and the site E is at the origin, as mentioned above. Then there are five possibilities for the choice of origin in the S1 phase. We call them *shift domains*. The structures with a different origin have the same atom positions but with a different Al and TM arrangement. They are also antiphase domains. The shift vector between the adjacent antiphase domains will be given by one of $\mathbf{x}_s = (s,s,s,s,5z)/5$ $(1 \leqslant s \leqslant 4)$. That is, they are related to each other by nonprimitive translations $\{E|\mathbf{x}_s\}$. In a completely ordered S1 phase, one of them appears but in some cases, we may expect a domain structure in the S1 phase where the domain volumes of these antiphase domains are different.

V. DIFFUSE SCATTERING DUE TO DISORDERED CLUSTERS

As mentioned in the previous two sections, there are 30 clusters in the S1 and b-Ni phases which occupy the vertices in the PPT, that is, C_k^{5f}, $C_k'^{5f}$, and C_k^m $(1 \leqslant k \leqslant 10)$. In order to apply the theory of the DS intensity formula mentioned below [see Eq. (4)] to these phases, the clusters C_k^{5f} $(1 \leqslant k \leqslant 10)$ are denoted by the indices μ from 1 to 10 in the following, and $C_k'^{5f}$ and C_k^m $(1 \leqslant k \leqslant 10)$ by μ from 11 to 20 and 21 to 30, respectively. The structure factor of the μth cluster is denoted by F^μ. The cluster distributions in the independent ODs are shown in Fig. 6.

To calculate the DS intensities of both phases, the coordinate system of the low-temperature phase with lattice constants of $a \simeq 5.2$ Å and $c \simeq 4.0$ Å are used in both phases.[24] In the following, the theory of DS intensity due to the disordered clusters is shortly summarized.

As shown in the previous paper,[7] the DS intensity due to disordered cluster orientations can be calculated by using the structure factor of the cluster in each orientation. When the structure factor of a (columnar) cluster is written as $F(\mathbf{q})$, that of the cluster related to it by an operator $\{R|\tau\}$ is given by $F(R^{-1}\mathbf{q})\exp(2\pi\mathbf{q}\cdot\tau)$.[30] Since a structure considered in this paper is completely periodic along the tenfold axis, $F(\mathbf{q})$

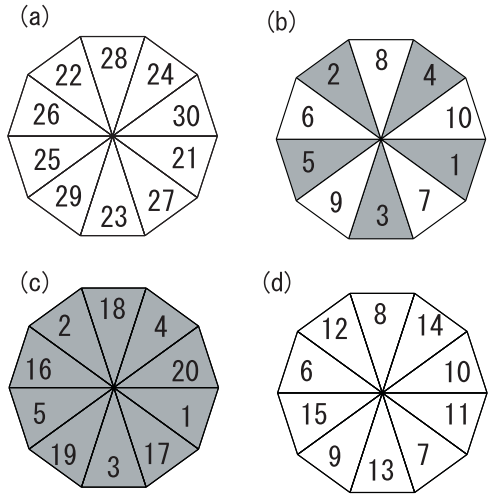

FIG. 6. Cluster distribution in the independent occupation domains (ODs) of cluster centers. (a) ODs in the b-Ni phase. (b), (c), and (d) ODs located at the E, A, and C sites in the S1 phase. The number indicates the cluster index μ (see text). The cluster distributions in the ODs at B and D sites are the same as those in (c) and (d) for the sites A and C, respectively. The sites generated by the gray and white ODs are occupied by the up and down orientation $5f$ clusters shown in Figs. 4(b) and 4(a) in an ideal S1 structure.

has an intensity only on a plane with $q_3 = n$ ($n = 0, \pm 1, \ldots$), where q_3 is the c* component of the diffraction vector $\mathbf{q}$ (in the external space). In the following, we consider the DS intensity on these layers. Then the DS intensity in these layers, *which is integrated along the tenfold axis*, is obtained by the structure factor of the atoms of a cluster within a period.

The DS intensity is expressed by the correlation function of the statistical variable z_i^μ, which takes 1 when the ith site is occupied by the μth cluster, otherwise 0.[7] Then the structure factor F_i for the ith site (the site generated by ith OD) is represented by $F_i = \sum_\mu F^\mu z_i^\mu = \sum_\mu F^\mu(\langle z_i^\mu\rangle + \Delta z_i^\mu)$. The first term $\sum_\mu F^\mu \langle z_i^\mu\rangle \equiv \langle F_i\rangle$ represents the average structure factor of the clusters which occupy the ith site. The fluctuation of the structure factor ΔF_i is defined by $\Delta F_i = \sum_\mu F^\mu \Delta z_i^\mu$. We denote the statistical variables for the clusters located at $\mathbf{x}_{i0}^e$ and $\mathbf{x}_{i'l}^e$ as z_{i0}^μ and $z_{i'l}^\nu$ and the structure factors of the cluster centered at these sites, as F_{0i}^μ and $F_{i'l}^\nu$.

The correlation function of the fluctuation of the cluster structure factors, $\langle \Delta F_{i0} \Delta F_{i'l}\rangle$, is given in terms of z_{i0}^μ and z_{il}^ν by

$$\langle \Delta F_{i0} \Delta F_{i'l}\rangle = \sum_{\mu\nu} F^\mu F^\nu \left\langle \Delta z_{i0}^\mu \Delta z_{i'l}^\nu \right\rangle, \tag{1}$$

where μ and ν run from 1 to 30 and

$$\begin{aligned} \left\langle \Delta z_{i0}^\mu \Delta z_{i'l}^\nu \right\rangle &= \left\langle z_{i0}^\mu z_{i'l}^\nu \right\rangle - \left\langle z_i^\mu \right\rangle \left\langle z_{i'}^\nu \right\rangle \\ &\equiv g_{ii'l}^{\mu\nu} \equiv -\left\langle z_i^\mu \right\rangle \left\langle z_{i'}^\nu \right\rangle \alpha_{ii'l}^{\mu\nu} \end{aligned} \tag{2}$$

is the correlation function of the fluctuation of z_{i0}^μ and $z_{i'l}^\nu$. The correlation function $g_{ii'l}^{\mu\nu}$ and the α parameter $\alpha_{ii'l}^{\mu\nu}$ depend on the external space component of the vectors $\Delta\mathbf{x}_{ii'l} \equiv \mathbf{x}_{i0} - \mathbf{x}_{i'l}$, so that they are explicitly written as $g_{ii'}^{\mu\nu}(\Delta\mathbf{x}_{ii'l}^e)$ and $\alpha_{ii'}^{\mu\nu}(\Delta\mathbf{x}_{ii'l}^e)$ in the following. They are assumed to decrease with the intercluster distance $|\Delta\mathbf{x}_{ii'l}^e|$. Using the correlation function and the structure factor of clusters, the DS intensity is given by[7]

$$\begin{aligned} I_D(\mathbf{q}) = -\kappa \sum_{ii'l} v_{ii'}\left(\Delta\mathbf{x}_{ii'l}^i\right) \left(\sum_{\mu>\nu} |\Delta F^{\mu\nu}|^2 g_{ii'}^{\mu\nu}\left(\Delta\mathbf{x}_{ii'l}^e\right) \right) \\ \times \exp\left(2\pi i \mathbf{q}\cdot\Delta\mathbf{x}_{ii'l}^e\right), \end{aligned} \tag{3}$$

where $\kappa = V/\Omega_n$, $\Delta F^{\mu\nu} \equiv F^\mu - F^\nu$, V is the volume of a quasicrystal (in the external space) while Ω_n denotes the unit cell volume of the decagonal lattice of the S1 phase. The frequency of the cluster center pairs (or vertex pairs of PPT in the present case) apart by $\Delta\mathbf{x}_{ii'l}^e = \mathbf{x}_{i0}^e - \mathbf{x}_{i'l}^e$ is proportional to $v_{ii'}(\Delta\mathbf{x}_{ii'l}^i)$, which is the overlapped area of the ODs of the cluster centers located at $\mathbf{x}_{i0}$ and $\mathbf{x}_{i'l}$ in 5D space when they are projected onto the 2D internal space. Therefore it is a function of the internal space component of $\Delta\mathbf{x}_{ii'l}$, $\Delta\mathbf{x}_{ii'l}^i$. In Eq. (3), i and i' run from 1 to 50, μ and ν run from 1 to 30, l runs lattice vectors which give rise to nonzero $v_{ij}(\Delta\mathbf{x}_{ijl}^i)$. (Note that for lattice vectors with large $|\Delta\mathbf{x}_{ii'l}^i|$, $v_{ii'}(\Delta\mathbf{x}_{ii'l}^i)$ vanishes. See Fig. 3 in Ref. 7.)

Using symmetry operations of a space group, Eq. (3) is rewritten as

$$\begin{aligned} I_D(\mathbf{q}) = -\kappa \sum_{ii'l} v_{ii'}\left(\Delta\mathbf{x}_{ii'l}^i\right) a_{ii'}(\Delta\mathbf{x}_{ii'l}) \sum_{\mu>\nu R} |R\Delta F^{\mu\nu}|^2 \\ \times g_{ii'}^{\mu\nu}\left(\Delta\mathbf{x}_{ii'l}^e\right) \exp\left(2\pi i \mathbf{q}\cdot R\Delta\mathbf{x}_{ii'l}^e\right), \end{aligned} \tag{4}$$

where $R\Delta F^{\mu\nu} \equiv F^\mu(R^{-1}\mathbf{q}) - F^\nu(R^{-1}\mathbf{q})$, i,i', and l run sites of independent OD pairs within the correlation length, R runs symmetry operations of the point group $10/mmm(10^71mm)$ and $a_{ii'}(\Delta\mathbf{x}_{ii'l})$ is the multiplicity of the OD pair, which is determined by the site symmetry of the ith and i'th ODs and the point group (see Appendix C). Thus if $v_{ii'}(\Delta\mathbf{x}_{ii'l}^i)$, $a_{ii'}(\Delta\mathbf{x}_{ii'l})$ and $g_{ii'}^{\mu\nu}(\Delta\mathbf{x}_{ii'l}^e)$ for independent cluster pairs together with the space group and the structure factor of clusters are known, the DS intensity is determined.

VI. CORRELATION OF CLUSTERS

As a model structure of a disordered b-Ni phase, we employ a microdomain model discussed in Sec. IV. In this model it is assumed that microdomains consisting of the antiphase domains of the S1 structure are created in the b-Ni phase, when the temperature approaches to T_c. A microdomain is considered to be one of the ten antiphase domains discussed in Sec. IV. The antiphase domains are assumed not to be correlated. The volume ratio of all antiphase domains is the same, that is, it is given by 1/10. In this case, the average structure of this disordered domain structure maintains the symmetry of the b-Ni phase. This ensures that there is no Bragg reflections at the satellite reflection positions of the S1 phase independent of the domain size whenever the domain size is less than the coherence length of x rays. However we can expect broad peaks at these positions which are coming from the antiphase domains (microdomains) with the structure of the S1 phase. The peak width of such a broad peak depends on the domain size. In the following, we consider the correlation within a range of the third nearest intercluster distance.

Soon after the phase transition from the b-Ni phase to the S1 phase, the existence of the antisymmetric domains is expected. However, the volume ratio of these domains should be different. One domain will become dominant after a time sufficiently long for growing dominant domains. In the following, we do not consider the shift domains in the S1 phase for simplicity but the possibility of the antisymmetric domains will be taken into account, since such antisymmetric domains are observed in d-Al-Ni-Fe, although this structure corresponds to the Co-rich phase of d-Al-Ni-Co.[31]

In the S1 phase, the microdomains having the structure of the b-Ni phase are assumed to be created near T_c to the b-Ni phase. In addition, it is assumed that the dissolution of $5f$ clusters at the sites E_k, A_k, B_k, C_k, and D_k creates m clusters, C_k^m. In the current model, these sites in two antisymmetric domains create the same m cluster, since the dissolution of C_k^{5f} and $C_k^{\prime 5f}$ creates C_k^m. Created m clusters are the same as those appearing in the ideal b-Ni phase. Such a model will approximate a case in which the intercluster correlation up to the third nearest cluster distances is taken into account. In contrast to the b-Ni phase, the created microdomains are correlated, since the structure in the microdomains is the same. Thus even if the microdomains are randomly distributed, inter-micro-domain correlations may exist. In the following, however, we do not take the inter-micro-domain correlations into account for simplicity.

In Eq. (4), we consider the self-correlation together with the intercluster correlation up to the third nearest clusters with intercluster vectors $\Delta\mathbf{x}_1$, $\Delta\mathbf{x}_2$, and $\Delta\mathbf{x}_3$ as $\Delta\mathbf{x}_{ii'l}$ and equivalent to them under the space group (see Table II). The corresponding intercluster distances are about 12, 20, and 32 Å. We employ the correlation function within these inter-cluster distances in the completely ordered phase as a correlation model.

In the zeroth approximation, the intercluster correlation is neglected. Then the self-correlation term mentioned later determines the DS intensity. In the next approximation, the intercluster correlations are taken into account.

Equation (4) includes only independent cluster-center pairs for each neighbor. They are generated by overlapped parts of the small triangles shown in Figs. 7(a)–7(c). These figures are obtained from Fig. 5(a) and another OD which is obtained from it by shifting by the internal space components of $\Delta\mathbf{x}_1$, $\Delta\mathbf{x}_2$, and $\Delta\mathbf{x}_3$, that is, $\Delta\mathbf{x}_1^i$, $\Delta\mathbf{x}_2^i$, and $\Delta\mathbf{x}_3^i$. Each overlapped

TABLE II. The area of overlapped occupation domains (OD) shown in Fig. 7. (The values for independent OD pairs are shown.) The two decagonal ODs are distant by the vectors listed in the first column. Each decagonal OD is subdivided into ten triangles with labels 1-10 shown in Fig. 5(a). The first, second, and third nearest cluster distances along $\mathbf{a}_1$ are given by the external space components of $\Delta\mathbf{x}_1 = (-1,4,4,-1,0)/5 = -(1,-1,-2,0,0)_0$, $\Delta\mathbf{x}_2 = -(-3,7,7,-3,0)/5 = (2,-2,-3,0,0)_0$, and $\Delta\mathbf{x}_3 = (-4,11,11,-4,0)/5 = -(3,-3,-5,0,0)_0$, respectively. The lengths of their external space components are $2a\tau^2/\sqrt{5}$, $2a\tau^3/\sqrt{5}$, and $2a\tau^4/\sqrt{5}$, respectively, while those of the internal space components are $2a\tau^{-2}/\sqrt{5}$, $2a\tau^{-3}/\sqrt{5}$, and $2a\tau^{-4}/\sqrt{5}$ (see Appendix A). The overlapped part of the ith and i'th triangles in the left and right decagonal ODs in Figs. 7(a), 7(b), or 7(c), when they are projected onto the internal space, is denoted by OD(i-i') in the second column. The third column shows the area of the overlapped part in the unit of the area of the triangle in Fig. 5, which is given by $2\tau^{-6}a^2/5\sin(\pi/5)$.

Vector	Overlapped part	Area
$\Delta\mathbf{x}_1$	OD(10-6)	τ^{-2}
$\Delta\mathbf{x}_2$	OD(4-2)	$2\tau^{-3}$
	OD(4-6),OD(10-2)	τ^{-2}
	OD(10-6)	τ^{-1}
$\Delta\mathbf{x}_3$	OD(8-2),OD(4-8)	τ^{-2}
	OD(4-2)	$2\tau^{-3}$
	OD(8-6),OD(10-8)	τ^{-3}
	OD(2-6),OD(10-4)	τ^{-3}
	OD(4-6),OD(10-2)	τ^{-4}
	OD(6-6),OD(10-10)	τ^{-4}
	OD(10-6)	τ^{-3}

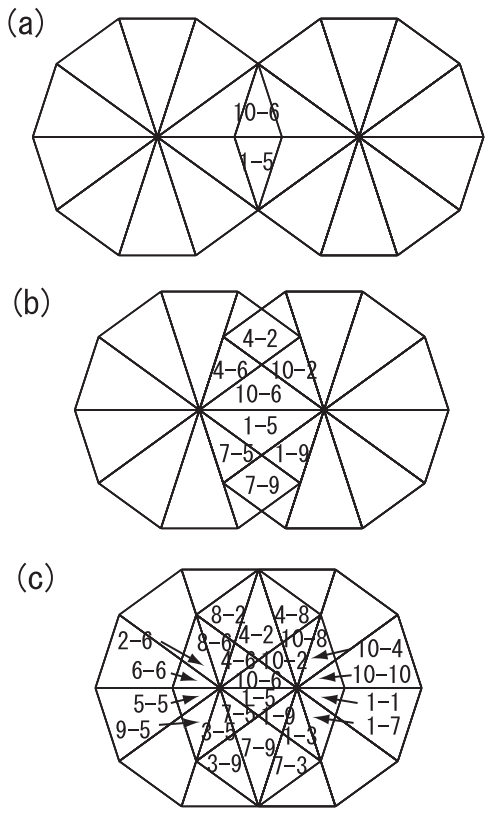

FIG. 7. Overlapped parts of two decagonal occupation domains for the three nearest cluster-center distances, after the projection of the two domains onto the internal space. (The horizontal and vertical directions are parallel to $\mathbf{a}_3$ and $\mathbf{a}_4$, respectively.) The two domains are distant by $\Delta\mathbf{x}_1$ (a), $\Delta\mathbf{x}_2$ (b), and $\Delta\mathbf{x}_3$ (c) (see Table II). The overlapped parts of the kth and k'th triangles in the left and right decagonal ODs labeled k-k' create the cluster center pairs distant from each other by $2\tau^2a/\sqrt{5} \simeq 12$ Å (a), $2\tau^3a/\sqrt{5} \simeq 20$ Å (b), and $2\tau^4a/\sqrt{5} \simeq 32$ Å (c) along the first axis $\mathbf{a}_1$. These intercluster distances correspond to the external space components of the three vectors, $\Delta\mathbf{x}_1^e$, $\Delta\mathbf{x}_2^e$, and $\Delta\mathbf{x}_3^e$, while the distances of the left and right ODs in (a), (b), and (c), to their internal space components, $\Delta\mathbf{x}_1^i$, $\Delta\mathbf{x}_2^i$, and $\Delta\mathbf{x}_3^i$. The independent cluster pair positions are generated by the labeled parts in the upper or lower half area. In the b-Ni phase, the parts labeled k-k' create the cluster centers which are occupied by the m clusters with kth and k'th orientations (see text).

part is denoted by $i - i'$ in Fig. 7 using the OD numbers in Fig. 5(a). The pairs only in an upper (or a lower) half part of Fig. 7(a) are, however, really independent as shown below.

A. Independent cluster pairs

In the b-Ni phase, the sites at $\mathbf{x}_s = (s,s,s,s,5z)/5$ ($0 \leqslant s \leqslant 4$) are translationally equivalent since they are a lattice vector of this phase as mentioned in Sec. IV. Their site symmetry is $\overline{10}m2(5mm)$ since the space group of the b-Ni phase is $P10_5/mmc(10^71mm)$. At each site, ten triangular ODs are situated sharing one corner (see Fig. 5). The site symmetry of each triangle is $2mm(mm1)$. [Note that in the b-Ni phase, the coordinate system is rotated by $\pi/10$ and a mirror plane in $\overline{10}m2(5mm)$ is on the normal from the center to an edge of the decagon, which divides the triangle into two similar triangles.] Since the site symmetry of an independent OD (a triangular OD) is low, there are many (ten in this case) equivalent ODs. Therefore independent pairs of these sites have to be considered. This means that there are ten independent cluster pairs in general for a fixed index i, since i' runs from 1 to 10. We consider ten cases where two ODs are distant by $R_5^n\Delta\mathbf{x}_j$, and $IR_5^n\Delta\mathbf{x}_j$ ($j = 1,2,3$ and $0 \leqslant n \leqslant 4$).

There are ten equidistant cluster pairs with a distance $|R_5^n\Delta\mathbf{x}_j| = |IR_5^n\Delta\mathbf{x}_j|$ ($0 \leqslant n \leqslant 4$) for each j. One of them is shown in Fig. 7 for the intercluster distance up to the third neighbors. The overlapped area $v_{ii'}(R_5^n\Delta\mathbf{x}_j)$ or $v_{ii'}(IR_5^n\Delta\mathbf{x}_j)$ is, however, zero for many pairs when $j = 1$, while many pairs give nonzero overlapped area for $j = 3$ as shown below.

We first consider possible pairs between OD 1 and other ODs with an intercluster vectors $\Delta\mathbf{x}_{ii'l} = R_5^n\Delta\mathbf{x}_1$ or $\Delta\mathbf{x}_{ii'l} = IR_5^n\Delta\mathbf{x}_1$. Noting that the internal space component of $\Delta\mathbf{x}_1$ is rotated by $4n\pi/5$ by R_5^n, and is inverted by I, the overlapped area is nonzero, only when $\Delta\mathbf{x}_{ii'l} = IR_5\Delta\mathbf{x}_1$ or $\Delta\mathbf{x}_{ii'l} = \Delta\mathbf{x}_1$ as is clear from Fig. 7(a). In the latter case, an OD pair OD($1-5$) has nonzero area. The intercluster vector in the internal space $IR_5\Delta\mathbf{x}_1^i$ is a vector which is obtained from $\Delta\mathbf{x}_1^i$ by the rotation of $-2\pi/10$. Then the OD 2 in a decagonal OD at this position is overlapped with OD 1 as is clear from Fig. 5(a). The OD ($1-2$) pair with the intercluster vector of $IR\Delta\mathbf{x}_1$ is equivalent to the OD pair ($10-6$) shown in Fig. 7(a) since the former is transformed to the latter by IR_5^3 in the point group $\overline{5}(\overline{5}^2)$ which generates all vectors equivalent to $\Delta\mathbf{x}_1$. At the same time the vector $IR_5\Delta\mathbf{x}_1$ is transformed to $\Delta\mathbf{x}_1$ by the same operator.

These two OD pairs are however related with $m(m)$ which leaves $\Delta\mathbf{x}_1$ invariant. Thus only one OD pair is independent. Other equivalent OD pairs are obtained from them by symmetry operators in the point group $\overline{5}m(\overline{5}^2m)$. A similar consideration concludes that there are four independent OD pairs in the second nearest intercluster distance, while there are 12 pairs in the third nearest intercluster distance. They are given by the labeled OD pairs in the upper half of Fig. 7. The areas of overlapped parts of these independent OD pairs are shown in Table II. The independent OD pairs can be determined by the site symmetry groups of two ODs and the group which leaves the intercluster distance $\Delta\mathbf{x}_i$ invariant (see Appendix C).

In the S1 phase, there are five translationally nonequivalent decagonal ODs denoted by E, A, B, C, and D, which are occupied by different clusters. Therefore, we need to consider different combinations of ODs for each case mentioned above. Since $\Delta\mathbf{x}_1 = \mathbf{x}_1 + (0,-1,-1,0,0)$, $\Delta\mathbf{x}_2 = \mathbf{x}_3 + (0,-2,-2,0,0)$, and $\Delta\mathbf{x}_3 = \mathbf{x}_4 + (0,-3,-3,0,0)$ (see Table II), that is, they are $\mathbf{x}_1$, $\mathbf{x}_2$, $\mathbf{x}_3$ plus a lattice vector of the S1 phase, the combinations of OD pairs for the inter-cluster distance $\Delta\mathbf{x}_1$ are A-E, B-A, C-B, D-C, and E-D, where A-E, etc., denote that the left and right decagonal ODs in Fig. 7 are ODs A and E, etc. Similarly, for $\Delta\mathbf{x}_2$, the possible combinations are C-E, D-A, E-B, A-C, and B-D. For $\Delta\mathbf{x}_3$, they are given by D-E, E-A, A-B, B-C, and C-D. Thus for each nearest neighbor, there are five possible combinations. (In b-Ni phase, E, A, B, C, and D sites are translationally equivalent. Therefore all the pairs are equivalent to E-E pair.)

B. Self-correlation of clusters

As the simplest approximation, we consider the DS intensity due to the self-correlation first. In this case, the correlation function is determined by $\langle\Delta z_i^\mu\rangle$. The nonzero self-correlation function is given by

$$g_{ii}^{\mu\nu}(\mathbf{0}) = \langle z_i^\mu\rangle\delta_{\mu\nu} - \langle z_i^\mu\rangle\langle z_i^\nu\rangle. \tag{5}$$

Since the DS intensity formulas Eqs. (3) and (4) include only $g_{ii'}^{\mu\nu}(\Delta\mathbf{x}_{ijl}^e)$ with $\mu \neq \nu$, the DS intensity is determined by $g_{ii}^{\mu\nu}(\mathbf{0}) = -\langle z_i^\mu\rangle\langle z_i^\nu\rangle$ ($\mu \neq \nu$). Then the α parameter is given by $\alpha_{ii}^{\mu\nu}(\mathbf{0}) = 1$ ($\mu \neq \nu$).

In the S1 phase, each vertex of the PPT is occupied by one of C_k^{5f} or $C_k^{\prime 5f}$ ($1 \leqslant k \leqslant 10$) in the completely ordered structure as mentioned in Sec. IV. When the index i is represented by $10s + k'$, ($0 \leqslant s \leqslant 4$ and $1 \leqslant k' \leqslant 10$), the indices $0 \leqslant s \leqslant 4$ indicate the sites $E_{k'}$, $A_{k'}$, $B_{k'}$, $C_{k'}$, and $D_{k'}$. On the other hand, $\mu = 10(\mu' - 1) + k$ ($1 \leqslant k \leqslant 10$ and $1 \leqslant \mu' \leqslant 3$) stand for C_k^{5f}, $C_k^{\prime 5f}$, or C_k^m for $\mu' = 1,2$, or 3, that is, the indices μ' and k represent the kind of clusters and their orientation. Then the occupation probability of the ith site, $\langle z_i^\mu\rangle$, is 1 only when $k = k'$ for $\mu' = 1$, or 2 in the completely ordered structure, otherwise, zero. In the disordered structure model, $\langle z_i^\mu\rangle$ becomes 2σ ($\sigma \leqslant 1/2$) for $k = k'$ ($1 \leqslant k \leqslant 10$) and $\mu' = 1$ or 2. At the same time, $\langle z_i^\mu\rangle$ for $\mu' = 3$ takes $(1 - 2\sigma)$, since C_k^{5f} or $C_k^{\prime 5f}$ partially dissolves and creates C_k^m with the same probability $(1 - 2\sigma)$.

Similarly, in the (disordered) b-Ni phase, $\langle z_i^\mu\rangle = (1 - 2\sigma)$ with $k = k'$, and $\mu' = 3$ and $\langle z_i^\mu\rangle = \sigma$ for $k = k'$ and $\mu' = 1$ or 2 for any k since C_k^m partially dissolves and creates C_k^{5f} and $C_k^{\prime 5f}$ with the probability σ.

In Eq. (4), we use $v_{ii}(\mathbf{0})$ as the unit of the area of a triangle in Fig. 5(a). Since the independent pair is only $(k,k) = (1,1)$ and its multiplicity is 1 (see Appendix C), the DS intensity due to the self-correlation, $I_D^0(\mathbf{q})$ in both b-Ni and S1 phases, is given by

$$I_D^0(\mathbf{q}) = -\kappa\sum_{s=0}^{4}\sum_{\mu'>\nu'R}|R\Delta F^{\mu\nu}|^2 g_{ii}^{\mu\nu}(\mathbf{0}), \tag{6}$$

where $i = 10s + k$, $\mu = 10(\mu' - 1) + k$, $\nu = 10(\nu' - 1) + k$ with $k = 1$ and μ' and ν' run values within the range $3 \geqslant \mu' > \nu' \geqslant 1$ and R runs symmetry operations of the point group $\overline{5}(\overline{5}^2)$. Because of different correlation function values in b-Ni

and S1 phases, intensity distributions are, however, different. Since the employed model of the S1 phase does not consider a correlation depending on the sublattices (indicated by the index s) and the sublattices are translationally equivalent in the b-Ni phase, each term in the above expression is the same for different s.

C. Intercluster correlation

The DS intensity due to the jth nearest intercluster correlation, $I_D^j(\mathbf{q})$, is given by

$$I_D^j(\mathbf{q}) = -\kappa \sum_{s=0}^{4} \sum_{(k,k')} v_{ii'}(\Delta \mathbf{x}_j) \sum_{\mu',\nu' R} |R\Delta F^{\mu\nu}|^2 \times g_{ii'}^{\mu\nu}\left(\Delta \mathbf{x}_j^e\right)\left[\exp\left(2\pi i \mathbf{q}\cdot R\Delta \mathbf{x}_j^e\right) + \text{c.c.}\right], \quad (7)$$

where $i = 10s + k$, $i' = 10s' + k'$, $\mu = 10(\mu' - 1) + k$, $\nu = 10(\nu' - 1) + k'$ and c.c. means the complex conjugate. μ' and ν' run $1 \leqslant \mu', \nu' \leqslant 3$ for $k \neq k'$ while they run values within the range $1 \leqslant \nu' < \mu' \leqslant 3$ for $k = k'$ and R runs all the operators in the point group $\bar{5}m(\bar{5}^2m)$. The combination of s and s' is fixed for each intercluster distance, that is, $s' = s + 1$, $s' = s + 3$, and $s' = s + 4$ (mod 5) for $j = 1,2$, and 3, respectively. For these pairs of s and s', 1, 4, or 12 pairs of k and k' are possible as shown Table II. Note that the multiplicity is one in the summation on the symmetry operation in Eq. (4) (see Appendix C).

D. Intercluster correlation in the b-Ni phase

Although a site is occupied by several clusters, the correlation function $g_{ii'}^{\mu\nu}(\Delta \mathbf{x}_{ii'l}^e)$ is nonzero only for the indices (μ,ν) mentioned above. In the current model, each site is occupied by one of three clusters, which are specific to the triangular ODs. For these combinations of (μ,ν), $g_{ii'}^{\mu\nu}(\Delta \mathbf{x}_{ii'l}^e)$ is different in general depending on the cluster distances, since the correlation between clusters in the S1 phase can be different for different $\Delta \mathbf{x}_{ii'l}^e$.

For the first neighbor, there is only one independent OD pair in the b-Ni phase, as shown in Table II. On the other hand, in the S1 phase there are five different OD pairs for this pair in the b-Ni phase. Corresponding to OD(10 − 6) in the b-Ni phase, there are five nonequivalent OD pairs, OD(10 − 46), OD(20 − 6), OD(30 − 16), OD(40 − 26), and OD(50 − 36). These i and i' are represented by $0 \leqslant s \leqslant 4$, $s' = s + 1$ and $(k,k') = (10,6)$. These OD pairs are occupied by the cluster pair specified by (μ,ν) with (10,6), (20,6), (20,16), (10,16), and (10,6), while these pairs are created by the dissolution of the cluster pairs (30,26). Note that the cluster pairs (10,6) (20,16) are parallel, while (20,6) and (10,16) are antiparallel. Therefore, parallel and antiparallel pairs appear 3 and 2 times, respectively.

In the second neighbor, the ODs at the site pairs C-E, D-A, E-B, A-C, and B-D have to be considered. The sites E, A, B, C, and D are occupied by up/down, up, up, down, and down orientation clusters in the S1 phase (see Fig. 6 and Appendix D). These give four antiparallel and one parallel cluster pairs for all the combinations of possible independent cluster pairs in this cluster distance. On the other hand, for the third intercluster neighbor, $s' = s + 4$ and this is equivalent to $s' = s - 1$ so that there are three parallel and two antiparallel pairs.

Accordingly, for the first and third neighbors, when an m cluster is dissolved and a $5f$ cluster is created with the occupation probability of σ, probabilities of pairs with parallel and antiparallel orientations are 3/5 and 2/5, respectively. On the other hand, they are 1/5 and 4/5 for the second neighbor. As mentioned before, we use a microdomain model where microdomains with the S1 phase structure are dispersed in the b-Ni phase. Then a $5f$ cluster appears only in the microdomains and the correlation within the domain is assumed to be complete up to the third intercluster neighbor. In this model, the correlation functions are given by those in either the ideal S1 phase or ideal b-Ni phase. The $5f$-cluster pairs appear only in the microdomains and the ten antiphase domains are assumed to be randomly distributed. When the m clusters are dissolved with the probability of 2σ, they create microdomains having ten antiphase domain structures in the S1 phase with the same probability $\sigma/5$. Then the correlation functions for the parallel and antiparallel $5f$-cluster pairs are given by $(3/5)\sigma(1-\sigma)$ and $(2/5)\sigma(1-\sigma)$ for the first case, while they are $(1/5)\sigma(1-\sigma)$ and $(4/5)\sigma(1-\sigma)$ in the second case. The cluster pairs $(\mu,\nu) = (20,26)$, (10,26), (30,6), (30,16) with $(\mu',\nu') = (1,3)$ or (2,3) appear neither in the S1 phase nor in the b-Ni phase, so that the correlation functions for $\mu = 1$, 2 and $\nu = 3$ or $\mu = 3$, and $\nu' = 1$, 2 are given by $-\sigma(1-2\sigma)$. The m cluster appears only in the b-Ni phase so that correlation function for $\mu = 3$ and $\nu = 3$ is $2\sigma(1-2\sigma)$. The correlation function values for possible combinations of (μ,ν) up to the third intercluster distances are given in Table III.

The total correlation is described by a 30×30 matrix for each cluster distance. This is, however, a 10×10 block matrix, each element of which is a 3×3 matrix. The kk' element of the block matrix denotes the correlation between the kth and k'th sites, where the three kinds of clusters, denoted by $\mu' = 1,2,3$ with the kth and k'th orientations are located. This block matrix is symmetric and includes many zero elements (3×3 zero matrices).

As shown in Table III, each element of the block matrix is a 3×3 symmetric matrix with a form

$$\begin{pmatrix} A_1 & A_2 & B \\ A_2 & A_1 & B \\ B & B & C \end{pmatrix}, \quad (8)$$

where $A_1 = \sigma(3/5 - \sigma)$, $A_2 = \sigma(2/5 - \sigma)$, $B = -\sigma(1 - 2\sigma)$, and $C = 2\sigma(1-2\sigma)$ for the first and third neighbors, while $A_1 = \sigma(1/5 - \sigma)$, $A_2 = \sigma(4/5 - \sigma)$, $B = -\sigma(1 - 2\sigma)$, and $C = 2\sigma(1-2\sigma)$ for the second neighbor. For $k = k'$, only the upper or lower triangular matrix excluding the diagonal part is necessary in the calculation of DS intensity.

E. Intercluster correlation in the S1 phase

In the b-Ni phase, an OD with index k was assumed to be occupied by C_k^m, C_k^{5f}, and $C_k^{\prime 5f}$. In particular, the occupation probabilities of the last two were the same because we consider the ten antiphase domains of the S1 with equal volume ratio appearing in the b-Ni phase. In contrast, in the S1 phase, the probabilities of C_k^{5f} and $C_k^{\prime 5f}$ for a fixed k are different in general.

TABLE III. The correlation functions and α parameters of the clusters in the b-Ni phase. The correlation functions $g_{ii'}^{\mu\nu}(\Delta\mathbf{x}) = g_{ii'}^{\nu\mu}(\Delta\mathbf{x})$ $(1 \leqslant i,i' \leqslant 50,\ 1 \leqslant \mu,\nu \leqslant 30)$ are nonzero only when $i = 10s + k$, $i' = 10s' + k'$, $\mu = 10(\mu' - 1) + k$, $\nu = 10(\nu' - 1) + k'$, $(0 \leqslant s \leqslant 4,\ 1 \leqslant k,k' \leqslant 10,\ 1 \leqslant \mu',\nu' \leqslant 3)$ for any s and s'. In addition to these conditions, the following conditions for s, s', k and k' have to be fulfilled. For $\Delta\mathbf{x} = \mathbf{0}$, $s = s'$, $k = k'$, while for $\Delta\mathbf{x} = \Delta\mathbf{x}_1$, $\Delta\mathbf{x}_2$, and $\Delta\mathbf{x}_3$, $s' = s + 1$, $s' = s + 3$, and $s' = s + 4$, (mod 5), respectively, and k and k' must be a number pair shown in Fig. 7. When $k \neq k'$, μ is not equal to ν independent of μ' and ν', even if $\mu' = \nu'$. Therefore the terms with $\mu' = \nu'$ in the table contribute to the diffuse scattering (DS) intensity. In contrast, they do not contribute to the DS intensity when $k = k'$ and $\mu' = \nu'$. [See Eqs. (3) and (4).] Such cases appear for $\Delta\mathbf{x} = \mathbf{0}$ and $\Delta\mathbf{x}_3$. The occupation probability of a dissolved m cluster in the b-Ni phase is given by 2σ. [$\xi_1 \equiv (3/5)(1-\sigma)$, $\xi_2 \equiv (2/5)(1-\sigma)$, $\xi_3 \equiv (1/5)(1-\sigma)$, $\xi_4 \equiv (4/5)(1-\sigma)$ and $\xi_5 \equiv (1-2\sigma)$.]

$\Delta\mathbf{x}$	$g_{ii}^{\mu\nu}(\Delta\mathbf{x})$,$a_{ii}^{\mu\nu}(\Delta\mathbf{x})$	$g_{ii}^{\mu\nu}(\Delta\mathbf{x})$,$a_{ii}^{\mu\nu}(\Delta\mathbf{x})$
	$\mu' = 2,\nu' = 1$	$\mu' = 3,\nu' = 1,2$
$\mathbf{0}$	$-\sigma^2$,1	$-\sigma\xi_5$,1
$\Delta\mathbf{x}$	$g_{ii'}^{\mu\nu}(\Delta\mathbf{x})$,$a_{ii'}^{\mu\nu}(\Delta\mathbf{x})$	$g_{ii'}^{\mu\nu}(\Delta\mathbf{x})$,$a_{ii'}^{\mu\nu}(\Delta\mathbf{x})$
	$\mu' = 2,\nu' = 1$	$\mu' = 3,\nu' = 1,2$
	$\mu' = 1,\nu' = 2$	$\mu' = 1,2,\nu' = 3$
$\Delta\mathbf{x}_1$	$\sigma\xi_2$,$-\sigma^{-1}\xi_2$	$-\sigma\xi_5$,1
$\Delta\mathbf{x}_2$	$\sigma\xi_4$,$-\sigma^{-1}\xi_4$	$-\sigma\xi_5$,1
$\Delta\mathbf{x}_3$	$\sigma\xi_2$,$-\sigma^{-1}\xi_2$	$-\sigma\xi_5$,1
$\Delta\mathbf{x}$	$g_{ii'}^{\mu\nu}(\Delta\mathbf{x})$,$a_{ii'}^{\mu\nu}(\Delta\mathbf{x})$	$g_{ii'}^{\mu\nu}(\Delta\mathbf{x})$,$a_{ii'}^{\mu\nu}(\Delta\mathbf{x})$
	$\mu' = \nu' = 1,2$	$\mu' = \nu' = 3$
$\Delta\mathbf{x}_1$	$\sigma\xi_1$,$-\sigma^{-1}\xi_1$	$2\sigma\xi_5$,$-2\sigma\xi_5^{-1}$
$\Delta\mathbf{x}_2$	$\sigma\xi_3$,$-\sigma^{-1}\xi_3$	$2\sigma\xi_5$,$-2\sigma\xi_5^{-1}$
$\Delta\mathbf{x}_3$	$\sigma\xi_1$,$-\sigma^{-1}\xi_1$	$2\sigma\xi_5$,$-2\sigma\xi_5^{-1}$

Then E_k, A_k, B_k, C_k, and D_k sites in the average structure are statistically occupied by C_k^{5f}, $C_k^{\prime 5f}$, and C_k^m. In the ideal structure of the S1 phase, they are occupied by one of C_k^{5f}, $C_k^{\prime 5f}$ as shown in Table I. In the S1 phase, even if two antisymmetric domains exist, their volume ratio has to be different. We call domains with larger and smaller volumes major and minor domains and denote their volume ratios as $\eta_1 \equiv (1+\eta)/2$ and $\eta_2 \equiv (1-\eta)/2$ $(0 \leqslant \eta \leqslant 1)$. (That is $\eta_1 + \eta_2 = 1$ independent of η.)

Two typical cases are conceivable, where the domain size of the major and minor antisymmetric domains is nearly equal to and much larger than that of the created m-cluster domains, which is the order of the third intercluster neighbor. In the former, even if there are no m clusters in the S1 phase, DS can be expected because of the short-range order in two antisymmetric domains and this is a highly disordered S1 structure. Therefore we consider only the latter case.

In the latter, we can consider the major and minor antisymmetric domains separately, neglecting the correlation between major and minor domains. We assume that the $5f$ clusters in the major and minor domains are dissolved with the same probability. Then the occupation probabilities of C_k^{5f} and $C_k^{\prime 5f}$ in these two domains are given by $\eta_1\xi$ and $\eta_2\xi$ with $\xi = 2\sigma$, respectively, while the total occupancy of C_k^m is $(1-2\sigma)$. The site $i = 10s + k$ in the S1 phase is occupied by C_k^{5f} or $C_k^{\prime 5f}$ depending on s in the major domain and C_k^{5f} and $C_k^{\prime 5f}$ are flipped in the minor domain. In the major domain, C_k^{5f} appear at ODs with $s = 0,1,2$ and $1 \leqslant k \leqslant 5$ and $s = 3,4$ and $6 \leqslant k \leqslant 10$, while in the minor domain $C_k^{\prime 5f}$ appear at the same ODs. Similarly $C_k^{\prime 5f}$ appear at ODs with $s = 1,2$ and $6 \leqslant k \leqslant 10$ $s = 0,3,4$ and $1 \leqslant k \leqslant 5$ in the major domain and $C_k^{\prime 5f}$ is replaced by C_k^{5f} in the minor domain. Therefore they are occupied by C_k^{5f} or $C_k^{\prime 5f}$ with different occupation probabilities.

We consider a case, where C_k^{5f} appear in the major domain. Then the 3×3 block matrix is given by

$$\begin{pmatrix} A_1 & A_2 & B_1 \\ A_2 & A_3 & B_2 \\ B_1 & B_2 & C \end{pmatrix}, \tag{9}$$

$A_1 = \eta_1\xi(1-\eta_1\xi)$, $A_2 = -\eta_1\xi\eta_2\xi$, $B_1 = -\eta_1\xi(1-\eta_1\xi-\eta_2\xi) = -\eta_1\xi 2\sigma$, $A_3 = \eta_2\xi(1-\eta_2\xi)$, $B_2 = -\eta_2\xi(1-\eta_1\xi-\eta_2\xi) = -\eta_2\xi 2\sigma$, $C = 2\sigma(1-2\sigma)$. In the other case where the C_k^{5f} is in the minor domain, the first and second lines and columns are swapped.

In the following, we consider the simplest case with $\eta = 1$ so that $\eta_1 = 1$ and $\eta_2 = 0$. Then the minor domain disappears. Let the major cluster in each site in an antisymmetric domain be a cluster in an ideal S1 phase shown in Figs. 6(b-d). Noting that the matrix elements in the second column and second line in Eq. (9) are zero, we can consider 2×2 matrix with a form

$$\begin{pmatrix} A & B \\ B & C \end{pmatrix}, \tag{10}$$

where $A = 2\sigma(1-2\sigma)$, $B = -2\sigma(1-2\sigma)$ and $C = 2\sigma(1-2\sigma)$. For $k = k'$, its upper (or lower) triangular part without the diagonal terms contributes to the DS. It should be noted that these correlation functions are independent of the site index s. The contribution of the pairs denoted by (k,k') with different s in Eq. (4), however, depends on s, because the ODs at kth domain with the domain number $i = 10s + k$ are occupied by different clusters as shown in Fig. 6 and accordingly $F^{\mu\nu}$ is different depending on s.

In the first intercluster distance, $s' = s + 1$ as mentioned in C. Then the cluster pairs to be considered for OD pairs specified by (i,i') with $(k,k') = (10,6)$ and $s' = s + 1$ are given by $(\mu',\nu') = (3,1)$, $(3,2)$, $(3,2)$, $(3,1)$, and $(3,1)$ for $s = 0,1,2,3,4$ and other combinations $(1,3)$,$(1,3)$, $(2,3)$, $(2,3)$, and $(1,3)$ for $s = 0,1,2,3,4$, since the clusters of the ODs at the sites B and D are equal to those at the sites A and C. (See Fig. 6.) Note that the latter combinations are equal to $(1,3)$, $(2,3)$, $(2,3)$, $(1,3)$, and $(1,3)$ for $s' = 0,1,2,3,4$ (mod 5). Similarly, for the second intercluster distances with $s' = s + 3$, the cluster pairs with $(k,k') = (4,2)$ have nonzero correlation function for $(\mu',\nu') = (3,2)$, $(3,2)$, $(3,1)$, $(3,1)$, $(3,1)$ for $s = 0,1,2,3,4$ and other ones for $s' = 0,1,2,3,4$ in which the first and second numbers are flipped. In both cases, cluster pairs with $(\mu',\nu') = (3,1)$ [or $(1,3)$] appear three times, while those with $(3,2)$ [or $(2,3)$], two times. This is because the ODs at the site E [Fig. 6(b)] are occupied only by clusters with $\mu' = 1$, while five among ten ODs at the sites A, B, C, and D are occupied by the clusters with $\mu' = 1$ and the other five by those with $\mu' = 2$ as is clear from Table I and Fig. 6. The same is true for

the ODs at sites B and D. Thus in each intercluster distance, three of five OD pairs with the same (k,k') and $s = 0,1,2,3,4$ are occupied by (3,1) cluster pairs and two of five by (3,2). Therefore the sum over s in Eq. (7) can be replaced by the sum over two terms with weights 3 and 2.

VII. DIFFUSE SCATTERING INTENSITY

Using the correlation functions given in the previous section, the DS intensity is calculated. Figures 8(a) and 8(b) show the DS intensities of b-Ni and S1 phases in the layers normal to the tenfold axis (zeroth Bragg layer) due to the self-correlation and correlations up to the third nearest intercluster distances in the case of $\sigma = 0.1$ and $\sigma = 0.4$, respectively, while Fig. 8(c) indicates the DS intensity of the S1 phase in the first Bragg layer for $\sigma = 0.4$. (To compare with reported DS patterns,[9,10,25] the x and y axes are taken to be parallel to the unit vectors $\mathbf{a}_1$ and $\mathbf{a}_2$ of the b-Ni phase.[24,30]) Figures 8(a) and 8(b) have similar DS intensity distributions but around the position shown by the arrows, the difference in DS intensity is clearly seen. A characteristic feature in both phases is that there are broad peaks at the position of the main and satellite reflection positions. Around the strong Bragg peak positions, ten broad peaks appear forming a decagon and they are linked by broad lines. (The strongest four Bragg reflection positions are shown in Fig. 9 by arrows.) Furthermore, there are many broad peaks forming ten pentagons around the decagon. Note that a similar intensity distribution linked by broad lines is seen in the S1 phase at 1120K. (See Fig. 2 in Ref. 25.) Thus the broad peaks observed at the satellite peak positions in the quenched b-Ni phase, and the broad peaks linked by broad lines observed in the S1 phase at 1120 K are reproduced by the current models, although the correlation models do not include adjustable parameters except for σ, so that agreement between the experimental and simulated results is not complete.

When only the self-correlation of the clusters is taken into account, the DS intensity in the S1 phase shows very broad peaks at several strong Bragg peak positions as shown in Fig. 9. These pattern will correspond to a case where clusters of the b-Ni phase are created in the S1 phase but they are randomly distributed without being correlated. In particular they do not form a micro cluster within which the constituent clusters are correlated. A similar DS pattern is obtained for the b-Ni phase, although detailed intensity distribution is slightly different because the respective correlation functions are different.

VIII. DISCUSSION

At the room temperature, the S1 phase shows DS which has very broad peaks at the position of several strongest Bragg peaks.[25] Such broad beaks are seen in the DS due to the self correlation (Fig. 9). The observed broad peaks are therefore considered to be due to the isolated 20 Å clusters with no correlation to each other. The DS of the S1 phase due to the self-correlation has been analyzed based on a different model. Kobas *et al*. assumed that some cluster centers are randomly occupied only by C_k^m $(1 \leqslant k \leqslant 10)$ with the same probability.[5] Then the DS due to the self-correlation is proportional to $\sum_{k=1}^{10} |F^\mu - \langle F \rangle|^2$ where $\mu = 20 + k$ $(1 \leqslant k \leqslant 10)$, F^μ is the structure factor of the m cluster with the kth orientation and

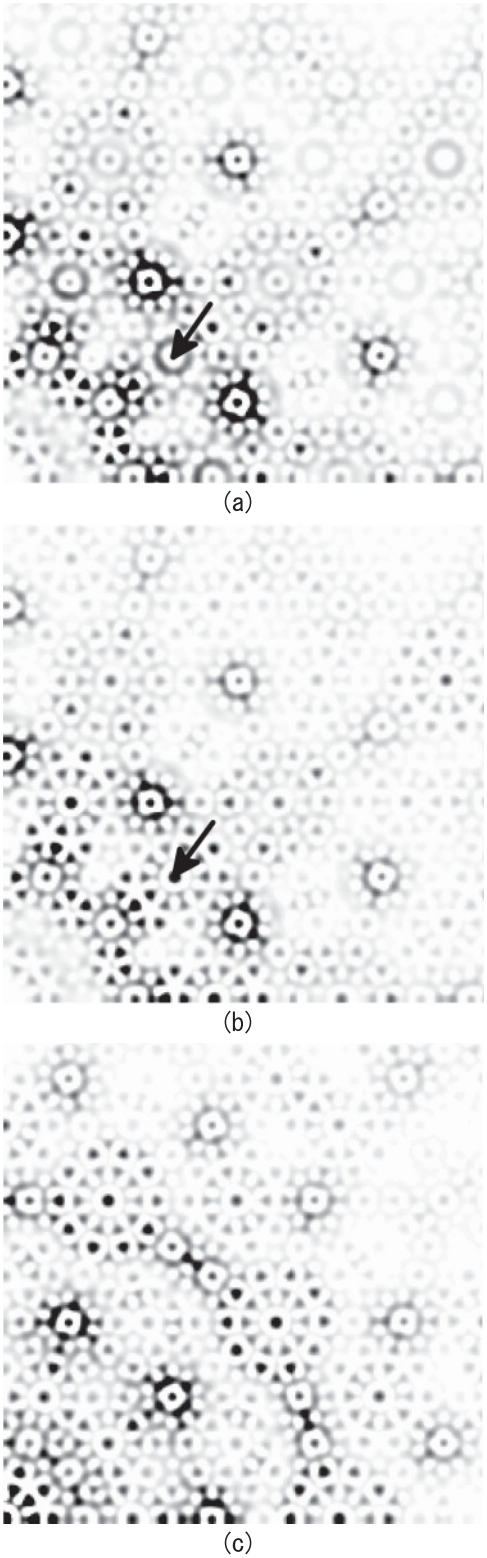

FIG. 8. The simulated diffuse scattering (DS) intensity calculated with the correlation up to the third nearest intercluster distances. The DS intensity distributions of the zeroth layer in the b-Ni phase (a) and the S1 phase (b) and that of the first layer in the S1 phase (c). (A quarter of each layer is shown. The origin is at the left bottom corner.) In the structure factor calculations of clusters, the isotropic temperature factor of 0.5 Å^2 was used for all atoms. (The intensity is proportional to darkness. $\sigma = 0.1$ for b-Ni and $\sigma = 0.4$ for S1 phases.)

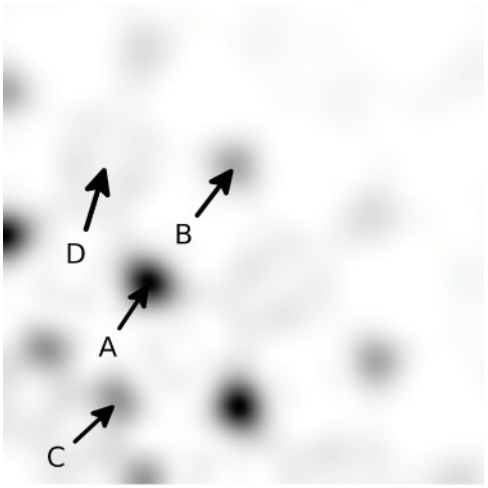

FIG. 9. Diffuse scattering intensity of the zeroth layer in the S1 phase calculated with only the self-correlation term given by Eq. (6). (A quarter of the layer is shown.) The arrows indicate the four strongest Bragg peak positions with indices 14410 (A), 37730 (B), 02210 (C), and 15630 (D). In Figs. 8(a) and 8(b), ten broad peaks are seen around these points and points equivalent to them. (The intensity is proportional to darkness.)

$\langle F\rangle = (1/10)\sum_{k=1}^{10} F^{\mu}$ is the average structure factor of the m clusters over ten different orientations.[5,7] In this model, the random arrangement of the $5f$ clusters is not taken into account. If some sites are statistically occupied by the $5f$ and m clusters, the structure factor of the $5f$ clusters has to be included in the DS intensity calculations. If some specific sites are preferentially occupied only by the m clusters, however, the situation assumed by the model is realized. One probable site may be site E, since this site is occupied by up and down orientation $5f$ clusters even in the completely ordered model of the S1 phase in contrast to other sites.

The broad peaks at the satellite reflection position in the quenched b-Ni phase[9] have to be explained by the correlation used. In the current model, the micro domains with the S1 structure are assumed to be created. In particular, the two $5f$ clusters in the second nearest intercluster distance in the S1 phase take antiparallel orientations preferentially. That is, among all cluster pairs with this distance, one-fifth of them takes both up or both down (parallel) orientations and four-fifths take the different orientation (antiparallel orientation) as stated in Sec. VI. This is considered to cause the broad peaks at the satellite reflection position.

In a previous paper, it was demonstrated that the DS intensities can be different for structures with the same average structure.[7] There is an opposite case where average structures are different but they give the same DS intensity. The average structure is determined by $\langle z_i^{\mu}\rangle$, provided that atom positions are the same. In Eqs. (6) and (7), if the correlation function $g_{ij'}^{\mu\nu}(\Delta\mathbf{x}_{ij'l})$ is the same for different $\langle z_i^{\mu}\rangle$, the DS intensity is the same. In the current model of the S1 phase, such a situation occurs. In Eq. (10), we have two solutions giving same A, B, and C. In the cases of $\sigma = 1/10$ and $2/5$, A is $4/25$. These two cases give the same DS intensity since $\mathrm{A} = -\mathrm{B} = \mathrm{C}$. That is, the average structures with $\sigma = 1/10$ and 2/5 are different, but their DS intensity is the same. Since 2σ represents the total occupation probability of the $5f$ clusters, in the former the m clusters are dominant, while in the latter the $5f$ clusters are dominant. Therefore the former may not be realistic as a model of the S1 phase. However, this result suggests that we can not deny the possibility of the same DS intensity for different structures in more realistic cases.

IX. SUMMARY AND CONCLUDING REMARKS

This paper demonstrated the effectiveness of a newly proposed theory by applying it to the analysis of short-range order diffuse scattering in quasicrystals. The quenched b-Ni phase and the S1 phase at 1120 K show characteristic DS intensity distribution. In the former, broad peaks exist with estimated correlation lengths of about 28 Å at the satellite reflection positions of the S1 phase. This is explained by the intercluster correlation of $5f$ clusters and m clusters with a diameter of $\simeq$20 Å up to the third intercluster distance ($\simeq$ 32 Å). The broad streaks observed at 1120 K in the S1 phase are also reproduced by similar intercluster correlations between $5f$ and m clusters up to the third intercluster neighbors. Very broad peaks at several strongest Bragg peaks in the S1 phase at room temper are considered to be due to isolated m clusters existing in this phase, since these peaks are reproduced by self-correlation terms. It was shown that the cluster-based DS analysis is applicable to the DS in b-Ni and S1 phases of d-Al-Ni-Co quasicrystals. This simplifies the DS intensity analysis drastically. These results suggest that the analysis of temperature dependent DS intensity will give important information of phase transition mechanism of quasicrystals.

APPENDIX A: COORDINATE SYSTEMS OF THE b-Ni AND S1 PHASES

The unit vectors $\mathbf{d}_i$ ($1 \leqslant i \leqslant 5$) of the 5D decagonal lattice of the S1 phase are defined by $\mathbf{d}_i = \sum_{j=1}^{5} \mathrm{R}_{ij}\mathbf{a}_j$ with [30]

$$\mathrm{R} = (2a/\sqrt{5})\begin{pmatrix} (c_1-1) & s_1 & (c_2-1) & s_2 & 0 \\ (c_2-1) & s_2 & (c_4-1) & s_4 & 0 \\ (c_3-1) & s_3 & (c_1-1) & s_1 & 0 \\ (c_4-1) & s_4 & (c_3-1) & s_3 & 0 \\ 0 & 0 & 0 & 0 & c\sqrt{5}/2a \end{pmatrix}, \tag{A1}$$

where $c_i = \cos(2\pi i/5)$ and $s_i = \sin(2\pi i/5)$, $\mathbf{a}_1$, $\mathbf{a}_2$, and $\mathbf{a}_5$ are the unit vectors in the external space, $\mathbf{a}_3$ and $\mathbf{a}_4$ are those in the internal space, and a and c are lattice constants of the decagonal lattice. The unit vectors of the reciprocal lattice in the b-Ni phase, $\mathbf{d}_{0i}^{*}$ ($i = 1,2,\ldots,5$), are expressed in terms of those of the S1 phase, $\mathbf{d}_i^{*}$, by $\mathbf{d}_{0i}^{*} = \sum_j \mathrm{S}_{ij}\mathbf{d}_j^{*}$,[15] where the matrix S is given by

$$\mathrm{S} = \begin{pmatrix} 1 & 0 & -1 & 0 & 0 \\ 0 & 1 & 0 & -1 & 0 \\ 1 & 1 & 2 & 1 & 0 \\ -1 & 0 & 0 & 1 & 0 \\ 0 & 0 & 0 & 0 & 1 \end{pmatrix}. \tag{A2}$$

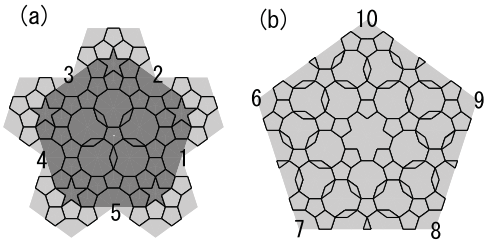

FIG. 10. Independent occupation domains of the b-Ni phase. These domains are located at $(1,1,1,1,5z)_0/5$ (a) and $(2,2,2,2,5z)_0/5$ ($z = 1/4$). The horizontal and vertical directions are parallel to $\mathbf{a}_4$ and $\mathbf{a}_5$ of the S1 phase. The size of the overlapped decagons are the same as that of the decagon in Fig. 5.

Therefore $\mathbf{d}_i^*$ are given by $\mathbf{d}_i^* = \sum_j \mathrm{T}_{ij}\mathbf{d}_{0j}^*$ with $\mathrm{T} = \mathrm{S}^{-1}$:

$$\mathrm{T} = \frac{1}{5}\begin{pmatrix} 2 & -1 & 1 & -2 & 0 \\ 2 & 4 & 1 & 3 & 0 \\ -3 & -1 & 1 & -2 & 0 \\ 2 & -1 & 1 & 3 & 0 \\ 0 & 0 & 0 & 0 & 5 \end{pmatrix}. \tag{A3}$$

The coordinates with respect to the two systems are transformed by the same matrices: $x_{0i} = \sum_j \mathrm{S}_{ij}x_j$ and $x_i = \sum_j \mathrm{T}_{ij}x_{0j}$.

APPENDIX B: ODS FOR THE CLUSTER CENTER WITH THE SAME LOCAL MIRROR SYMMETRY

The subdivision of decagonal ODs in Fig. 5 comes from the fact that lower symmetric ODs labeled 1-5 in Fig. 10(a) located at $(1,1,1,1,5z)_0/5$ and corresponding parts in the inverted OD at $-(1,1,1,1,5z)_0/5$ generate seven atom positions in the second nearest atom positions from the cluster center in the b-Ni phase shown in Fig. 3. [The decagons in Figs. 10(a) and 10(b) have the same size as the OD of the cluster center shown in Fig. 5.] On the other hand, three first nearest neighbor positions are created by ODs 6–10 in Fig. 10(b) and the corresponding parts of the inverted OD at $-(2,2,2,2,5z)/5$.[24] Note that the area of the ODs 1–5 is 7/10 of that of the cluster center OD, while the area of the ODs 6–10 is 3/10. This leads to the subdivision of ODs for the cluster centers shown in Fig. 5.

APPENDIX C: MULTIPLICITY OF OD PAIRS IN THE INTENSITY FORMULA

The multiplicity $a_{ij}(\Delta\mathbf{x}_{ii'l})$ in Eq. (4) is determined by the order of a group which is given by an intersection of three groups mentioned below. Let the site symmetries of the ith and i'th ODs be G_1 and G_2 and a subgroup of G, which leaves $\Delta\mathbf{x}_{ii'l}$ invariant, be G_3. Then there are N/N_1 and N/N_2 sites equivalent to the ith and i'th sites, where N_1, N_2, and N are the orders of G_1, G_2, and the point group G.

We consider the intersection (common group) of G_1, G_2, and G_3 and denote it as $G_c = G_1 \cap G_2 \cap G_3$. Then equivalent pairs are generated by the left coset representatives g_i of G in $G = \sum_i g_i G_c$. The number of coset representatives is equal to N/N_c, where N_c is the order of G_c. The multiplicity of an OD pair distant by $\Delta\mathbf{x}_{ii'l}$ is therefore given by N_c/N. (When G_c is a normal subgroup of G, the order of the factor group G/G_c is equal to N/N_c.)

A site symmetry operation of an OD transforms the OD into itself. This means that the shape of the OD has to be invariant under the site symmetry group, in contrast to a conventional crystal where the symmetry of an atom is assumed to be equal to or higher than the site symmetry. In general, the symmetry of an OD is lower than or equal to the symmetry of its corner or center (of gravity) position. In the case of triangular ODs, E_k, A_k, etc., they have the point symmetry (point group) $2mm(mm1)$, since all ODs are on the mirror plane normal to the tenfold axis, although the site symmetry of one corner (center of the decagon) is $\bar{1}0m2$. In this case, the site symmetry group of each triangular OD, G_i ($i = 1,2$), is $2mm(mm1)$ and G_3 for $\Delta\mathbf{x}_{ii'l} = \Delta\mathbf{x}_i$ ($i = 1,2,3$) is $2mm(mm1)$. Their order is 4. The directions of $2(m)$ or $m(m)$ in these point groups for E_k, A_k, etc., with different k are different, so that their intersection becomes $m(1)$, the mirror plane of which is normal to the tenfold axis. This is a normal subgroup of the point group $10/mmm(10^71mm)$ and its order is 2. When the indices k of both ODs are the same, the intersection $G_1 \cap G_2$ is $2mm(mm1)$ but even in this case, $G_1 \cap G_2 \cap G_3$ is $m(1)$. Therefore $N/N_c = 20$, since the order N of the point group $10/mmm(10^71mm)$ is 40. This means that there are 20 OD pairs equivalent to each independent OD pair and its multiplicity $a_{ii'}(\Delta\mathbf{x}_{ii'l})$ is 1/2. In this case, the factor group for all independent OD pairs is isomorphic to $\bar{5}m(\bar{5}^2m)$ and we can choose elements in $\bar{5}m(\bar{5}^2m)$ as the coset representatives.

On the other hand for $\Delta\mathbf{x}_{ii'l} = \mathbf{0}$, G_1 and G_2 are equal and $G_1 \cap G_2 = 2mm(mm1)$, while $G_3 = 10/mmm(10^71mm)$, so that the intersection $G_c = G_1 \cap G_2 \cap G_3$ is $2mm(mm1)$. (Note that this is not a normal subgroup of the point group.) In this case we can choose elements in $\bar{5}(\bar{5}^2)$ as the coset representatives and the number of coset representatives is $N/N_c = 10$. Therefore the multiplicity is 1/4. [Note that $G = \sum_{i=1}^4 g_i G_q = \sum_{i=1}^4 G_q g_i$, where $G_q = \bar{5}(\bar{5}^2)$ and g_i ($i = 1,2,3,4$) are elements of G_c.]

Instead of using all symmetry operations in the point group in the summation with respect to R in Eq. (4), we can use the coset representatives mentioned above in order to avoid redundant calculations. Then the multiplicity is 1 although the coset representatives are different dependent on the OD pairs and $\Delta\mathbf{x}_{ii'l}$ in general as mentioned above. This fact is used in Eqs. (6) and (7). In practical calculations, we used R in the group $\bar{5}m(\bar{5}^2m)$ in all intercluster distances in Eq. (4). Then the multiplicities are 1 and 1/2 for $\Delta\mathbf{x}_{ii'l} = \Delta\mathbf{x}_i$ and $\mathbf{0}$.

APPENDIX D: ORIENTATION OF 5f CLUSTERS IN THE S1 PHASE

The location of small ODs in Fig. 1 is conveniently represented by a 6D representation of a 5D vector. The 6D representation of a 5D vector $\mathbf{x} = (y_1,y_2,y_3,y_4,y_5,y_6)$ is defined by $\mathbf{x} = \sum_{j=1}^6 y_i\mathbf{e}_j$, where

$$\mathbf{e}_i = (2a/\sqrt{5})(c_i\mathbf{a}_1 + s_i\mathbf{a}_2 + c_{2i}\mathbf{a}_3 + s_{2i}\mathbf{a}_4) \quad (1 \leqslant j \leqslant 5),$$
$$\mathbf{e}_6 = \mathbf{a}_5. \tag{D1}$$

Then the unit vectors $\mathbf{d}_j$ $(1 \leqslant j \leqslant 5)$ of the decagonal lattice are given in terms of $\mathbf{e}_i$ by

$$\mathbf{d}_j = \mathbf{e}_j - \mathbf{e}_5 \quad (1 \leqslant j \leqslant 4), \qquad \mathbf{d}_5 = \mathbf{e}_6. \tag{D2}$$

(See Appendix A.) Therefore 5D coordinates (x_1,x_2,x_3,x_4,x_5) of a 5D vector are obtained from its 6D representation by $x_i = \sum_{j=1}^{6} M_{ij} y_j$ with a 5×6 matrix M:

$$M = \frac{1}{5}\begin{pmatrix} 4 & -1 & -1 & -1 & -1 & 0 \\ -1 & 4 & -1 & -1 & -1 & 0 \\ -1 & -1 & 4 & -1 & -1 & 0 \\ -1 & -1 & -1 & 4 & -1 & 0 \\ 0 & 0 & 0 & 0 & 0 & 5 \end{pmatrix}. \tag{D3}$$

The 6D representations of the position of ODs 0-4 in Fig. 1 from the center at $\mathbf{x}_0 = (0,2,-1,1,0)/5$ are given by $\mathbf{y}_0 = (0,-2,1,-1,2,0)^i/5$, $\mathbf{y}_1 = (2,0,-2,1,-1,0)^i/5$, $\mathbf{y}_2 = (-1,2,0,-2,1,0)^i/5$, $\mathbf{y}_3 = (1,-1,2,0,-2,0)^i/5$, and $\mathbf{y}_4 = (-2,1,-1,2,0,0)^i/5$. [Note that latter four are obtained from the first one by the cyclic permutation of elements y_i $(1 \leqslant i \leqslant 5)$.]

Accordingly the 5D coordinates of $\mathbf{y}_j$ $(0 \leqslant j \leqslant 4)$ are given by $\mathbf{y}_0 = (0,-2,1,-1,0)^i/5 = (-1,-1,-1,-1,0)^i_0/5$, $\mathbf{y}_1 = (2,0,-2,1,0)^i/5 = (4,-1,-1,-1,0)^i_0/5$, $\mathbf{y}_2 = (-1,2,0,-2,0)^i/5 = (-1,4,-1,-1,0)^i_0/5$, $\mathbf{y}_3 = (1,-1,2,0,0)^i/5 = (-1,-1,4,-1,0)^i_0/5$, and $\mathbf{y}_4 = (-2,1,-1,2,0)^i/5 = (-1,-1,-1,4,0)^i_0/5$. The vectors $\mathbf{y}_j$ $(j = 1,2,3,4)$ are obtained from $\mathbf{y}_0$ by fivefold rotations: $\mathbf{y}_j = R_5^j \mathbf{y}_0$. Similarly, the vectors obtained from $\mathbf{x}_0$ by fivefold rotations are given by $R_5\mathbf{x}_0 = (-2,0,2,-1,0)/5$, $R_5^2\mathbf{x}_0 = (1,-2,0,2,0)/5$, $R_5^3\mathbf{x}_0 = (-1,1,-2,0,0)/5$, and $R_5^4\mathbf{x}_0 = (2,-1,1,-2,0)/5$, at which rotated ODs are located.

When $\mathbf{x} = \mathbf{y}$ modulo a lattice vector is written as $\mathbf{x} \equiv \mathbf{y}$, the relations $R_5^j\mathbf{x}_0 - \mathbf{x}_0 \equiv \mathbf{x}_k$ $(1 \leqslant j \leqslant 4,\ k = 3j \bmod 5)$ hold. [In fact we obtain $R_5^j\mathbf{x}_0 - \mathbf{x}_0 = \mathbf{x}_k + \Delta\mathbf{X}_j$ with $\Delta\mathbf{X}_1 = (-1,-1,0,-1,0)$, $\Delta\mathbf{X}_2 = (0,-1,0,0,0)$, $\Delta\mathbf{X}_3 = (-1,-1,-1,-1,0)$, and $\Delta\mathbf{X}_4 = (0,-1,0,-1,0)$.] Then we have $R_5^l(\mathbf{x}_0 + R_5^j\mathbf{y}_0) \equiv R_5^{l+j}\mathbf{x}_0^e - \mathbf{x}_k$ $(0 \leqslant l \leqslant 4)$. (Note that $R_5\mathbf{x}_k \equiv \mathbf{x}_k$.) This means that if the ODs at $\mathbf{x}_0 + R_5^j\mathbf{y}_0$ are occupied by TM or Al, TM or Al are located at $R_5^{l+j}\mathbf{x}_0^e$ from the cluster centers which are generated by ODs at $-\mathbf{x}_k$. This leads to the arrangement of clusters. For the cluster centers generated by ODs A, B, C, and D, the $5f$ clusters located at these sites take up, up, down, and down orientations, respectively. For sites generated by OD E, $5f$ clusters take up and down orientations depending on the site. When the site is generated by ODs with labels 1–5 in Fig. 6(b), the cluster has an up orientation, while for the site generated by ODs with labels 6–10, it takes a down orientation.

[1] M. V. Jarić and D. R. Nelson, Phys. Rev. B **37**, 4458 (1988).
[2] J. Lei, R. Wang, C. Hu, and D.-H. Ding, Phys. Rev. B **59**, 822 (1999).
[3] Y. Ishii, Mater. Sci. Eng. **294**, 377 (2000).
[4] M. M. D. Boissieu, M. Boudard, B. Hennion, R. Bellissent, S. Kycia, A. Goldman, C. Janot, and M. Audier, Phys. Rev. Lett. **75**, 89 (1995).
[5] M. Kobas, T. Weber, and W. Steurer, Phys. Rev. B **71**, 224206 (2005).
[6] H. Abe, K. Yamamoto, S. Matsuoka, and Y. Matsuo, J. Phys. Condens. Matter **19**, 466201 (2007).
[7] A. Yamamoto, Acta Crystallogr. Sect. A **66**, 372 (2010).
[8] F. Frey and W. Steurer, J. Non-Cryst. Solids **153–154**, 600 (1993).
[9] H. Abe, Y. Matsuo, H. Saitoh, T. Kusakake, K.-i. Ohshima, and H. Nakao, Jpn. J. Appl. Phys. **39**, L1111 (2000).
[10] H. Abe, T. Ueno, H. Nakao, Y. Matsuo, K. Ohshima, and H. Masumoto, J. Phys. Condens. Matter **15**, 1665 (2003).
[11] E. Weidner, F. Frey, J.-L. Lei, B. Pedersen, C. Paulmann, and W. Morgenroth, J. Appl. Crystallogr. **37**, 802 (2004).
[12] W. Steurer, Z. Kristallogr. **219**, 391 (2004).
[13] M. J. Capitan, Y. Calvayrac, A. Quivy, J. L. Joulaud, S. Lefebvre, and D. Gratias, Phys. Rev. B **60**, 6398 (1999).
[14] N. Shramchenko, H. Klein, R. Caudron, and R. Bellissent, Mater. Sci. Eng. A **294–296**, 335 (2000).
[15] K. Edagawa, M. Ichihara, K. Suzuki, and S. Takeuchi, Philos. Mag. Lett. **66**, 19 (1992).
[16] S. Ritsch, H. U. Nissen, and C. Beeli, Phys. Rev. Lett. **76**, 2507 (1996).
[17] S. Ritsch, C. Beeli, H. U. Nissen, T. Godecke, M. Scheffer, and R. Lück, Philos. Mag. Lett. **78**, 67 (1998).
[18] H. Takakura, A. Yamamoto, and A. P. Tsai, Acta Crystallogr. Sect. A **57**, 576 (2001).
[19] H. Takakura, A. Yamamoto, and A. P. Tsai, Ferroelectrics **305**, 257 (2004).
[20] T. Janssen, J. L. Birman, V. A. Koptsik, M. Senechal, D. Weigel, A. Yamamoto, and S. C. Abrahams, Acta Crystallogr. Sect. A **55**, 761 (1999).
[21] T. Janssen, J. L. Birman, F. Denoyer, V. A. Koptsik, J. L. Verger-Gaugry, D. Weigel, A. Yamamoto, and S. C. Abrahams, Acta Crystallogr. Sect. A **58**, 605 (2002).
[22] K. Saitoh, K. Tsuda, and M. Tanaka, Philos. Mag. A **76**, 135 (1997).
[23] K. Saitoh, K. Tsuda, M. Tanaka, A. P. Tsai, A. Inoue, and T. Masumoto, J. Phys. Soc. Jpn. **73**, 1786 (2004).
[24] A. Yamamoto, H. Takakura, and E. Abe, Phys. Rev. B **72**, 144202 (2005).
[25] M. Kobas, T. Weber, and W. Steurer, Phys. Rev. B **71**, 224205 (2005).
[26] E. Abe, K. Saitoh, H. Takakura, A. P. Tsai, P. J. Steinhardt, and H. C. Jeong, Phys. Rev. Lett. **84**, 4609 (2000).
[27] B. E. Warren, B. L. Averbach, and B. W. Roberts, J. Appl. Phys. **22**, 1493 (1951).
[28] H. Takakura, A. Yamamoto, and A. P. Tsai, Mater. Res. Soc. Sym. Proc. **643**, K9.9.1 (2001).
[29] A. Yamamoto, Philos. Mag. **87**, 3067 (2007).
[30] A. Yamamoto, Acta Crystallogr. Sect. A **52**, 509 (1996).
[31] K. Tsuda, M. Saito, M. Terauchi, M. Tanaka, A. P. Tsai, A. Inoue, and T. Masumoto, Jpn. J. Appl. Phys. **32**, 129 (1993).